disease severity (5). Further, enhanced production of free radicals has been shown to increase the production of hyaluronan, which is a major glycosaminoglycan component of the ECM and has been identified as an endogenous ligand for Toll-like receptors (TLRs), leading to inflammatory responses (9).

The bleomycin-induced SSc model in mice is established using subcutaneous bleomycin treatment (10). This treatment induces skin fibrosis and pulmonary fibrosis, which are central features of human SSc (10–13). Recent studies have revealed that bleomycin induces oxidative stress: in bleomycin-induced lung fibrosis, inflammatory cells and lung epithelial cells are responsible for free radical production (14). In addition, $p47^{phox-/-}$ mice, which are deficient in free radical production through the NADPH oxidase pathway, exhibit reduced bleomycin-induced lung fibrosis, suggesting that generation of free radicals by bleomycin induces tissue damage and fibrosis (15). Another model of SSc is the tight skin mouse model, which is a genetic animal model for the human disease. The tight skin mutation was originally identified as a spontaneous mutation that results in increased synthesis and excessive accumulation of collagen and other ECM proteins and autoantibody production (12,13). Previous studies have shown that antioxidants are reduced in TSK/+ mice (16), which suggests that oxidative stress contributes to fibrosis and immunologic abnormalities in these animals, as in human SSc patients.

Edaravone (3-methyl-1-phenyl-2-pyrazolin-5-one) is a free radical scavenger and a novel neuroprotective agent used in the treatment of acute embolic stroke in humans (17). This drug can scavenge not only hydroxyl radicals but also other free radicals, such as peroxynitrite radicals generated from nitric oxide (NO) (18). Under physiologic conditions, 50% of edaravone is present in anion form. Edaravone anion releases electrons that exert radical scavenging (17,18). Subsequently, edaravone radicals are generated. They react readily with oxygen atoms and eventually form 2-oxo-3-(phenylhydrazono) butanoic acid. We therefore hypothesized that, because SSc is likely caused by free radicals, it may be attenuated by edaravone. To test this hypothesis, in the present study we assessed the therapeutic effects of edaravone on fibrosis in mice with bleomycin-induced SSc and in TSK/+ mice and evaluated its association with immunologic abnormalities. We found that edaravone treatment ameliorated fibrosis both in mice with bleomycin-induced SSc and in TSK/+ mice. Our results suggest that edaravone has potential as a therapeutic agent for SSc.

MATERIALS AND METHODS

Mice. TSK/+ mice on a C57BL/6 genetic background and wild-type C57BL/6 mice were purchased from The Jackson Laboratory. To verify the TSK/+ genotype, polymerase chain reaction (PCR) amplification of a partially duplicated fibrillin 1 gene was conducted using genomic DNA from each mouse, as previously described (12). All studies and procedures were approved by the Committee on Animal Experimentation of Nagasaki University Graduate School of Medical Science.

Bleomycin-induced SSc. Bleomycin (Nippon Kayaku) was dissolved in phosphate buffered saline (PBS) at a concentration of 1 mg/ml and sterilized by filtration. Bleomycin or PBS (300 μg) was injected subcutaneously into the shaved back of the wild-type C57BL/6 mice daily for 4 weeks, as described previously (11).

Edaravone treatment. Edaravone (Tanabe-Mitsubishi) dissolved in sterile saline solution was administered intravenously into the tail vein of wild-type mice used in the studies of bleomycin-induced SSc and TSK/+ mice, for 28 days at a dose of 1.5 mg/kg/day (17–20). For the studies of bleomycin-induced SSc, edaravone treatment was administered just prior to bleomycin treatment each day. Control TSK/+ and wild-type mice were treated with saline. Treatment was started when the mice were 6 weeks old, with 10 mice in each treatment group. At least 3 independent experiments were performed for each assay. Edaravone- or saline-treated TSK/+ and wild-type mice were healthy, fertile, and did not display any evidence of infection or disease. According to postmarketing surveillance, edaravone can induce renal damage (21), and therefore, the kidneys of edaravone-treated wild-type and TSK/+ mice were examined histopathologically to assess for adverse effects. In this study, there was no sign of kidney toxicity from edaravone.

Histopathologic assessment of dermal and hypodermal fibrosis. Morphologic characteristics of skin sections were assessed by light microscopy. All skin sections were obtained from the para-midline, lower back region after 1, 2, 3, or 4 weeks of edaravone treatment. Sections were stained with hematoxylin and eosin (H&E). Dermal thickness (defined as the thickness of skin from the top of the granular layer to the junction between the dermis and subcutaneous fat) and hypodermal thickness (determined by measuring the thickness of the subcutaneous connective tissue beneath the panniculus carnosus) were examined. All of the sections were examined independently by 2 investigators (AY and SS), under blinded conditions. Because similar results were obtained when male and female mice were analyzed separately, skin thickness data from female mice only were used in this study. Neutrophils were identified by H&E staining and were counted in 10 random grids by light microscopy under high magnification (400×).

Histopathologic assessment of lung fibrosis. Lungs were excised from mice with bleomycin-induced SSc after 1, 2, 3, or 4 weeks of treatment with edaravone and stained with H&E and van Gieson's stain to detect collagen (11,12). The severity of lung fibrosis was assessed semiquantitatively as described by Ashcroft et al (22). Briefly, fibrosis was graded on a scale of 0–8 by examining randomly chosen fields of the left middle lobe at a magnification of 100×. Grading criteria were

as follows: grade 0 = normal lung; grade 1 = minimal fibrous thickening of alveolar or bronchiolar walls; grade 3 = moderate thickening of walls without obvious damage to lung architecture; grade 5 = increased fibrosis with definite damage to lung structure and formation of fibrous bands or small fibrous masses; grade 7 = severe distortion of structure and large fibrous areas; and grade 8 = total fibrous obliteration of fields. Grades 2, 4, and 6 were used for findings that were intermediate between the above-described features.

Immunohistochemical staining. Frozen skin tissue sections were incubated with rat monoclonal antibody specific for macrophages (F4/80 [Serotec], B220 [BD PharMingen], and CD3 [clone 145-2C11; BD PharMingen]). Rat IgG (Southern Biotechnology Associates) was used as a control for nonspecific staining. Sections were sequentially incubated with biotinylated rabbit anti-rat IgG secondary antibody (Vectastain ABC method; Vector). Stained sections and cells were counted in 10 random grids by light microscopy under high magnification (400×).

Determination of hydroxyproline content in the skin and lung tissue. Hydroxyproline is a modified amino acid that is uniquely found in high proportion in collagen. Therefore, skin and lung tissue hydroxyproline content was determined as a quantitative measure of collagen deposition, as previously described (12). Punch biopsy samples (6 mm) obtained from shaved dorsal skin and the harvested right lung of each mouse were analyzed. A hydroxyproline standard solution of 0–6 mg/ml was used to generate a standard curve.

Serum levels of cytokines, hyaluronan, H_2O_2, NO, immunoglobulins, and autoantibodies. Sera were obtained by cardiac puncture after 4 weeks of treatment with edaravone. Serum levels of interleukin-6 (IL-6), transforming growth factor β1 (TGFβ1), tumor necrosis factor α (TNFα), interferon-γ (IFNγ), and hyaluronan were assessed using specific enzyme-linked immunosorbent assay (ELISA) kits according to the protocols described by the manufacturer (R&D Systems). Serum production of H_2O_2 was determined using an H_2O_2 colorimetric assay kit (StressGen). Serum levels of NO were measured with a nitrite/nitrate colorimetric assay kit (Cayman Chemical). Serum Ig concentrations were assessed as previously described (12), using affinity-purified mouse IgM, IgG1, IgG2a, IgG2b, and IgG3 (Southern Biotechnology Associates) to generate standard curves. A specific ELISA kit (Medical and Biological Laboratories) was used to measure anti–topoisomerase I (anti–topo I) antibodies.

RNA isolation and real-time PCR. The dorsal skin punch biopsy samples and the harvested left lungs were homogenized in 0.1*M* Tris (pH 7.4) containing 1 m*M* EDTA and 10 μM indomethacin. Total RNA from the lower back skin and the lung was isolated with RNeasy spin columns (Qiagen) and reverse-transcribed onto complementary DNA. Expression of IL-6, TGFβ1, TNFα, and IFNγ was analyzed with an ABI Prism 7000 Sequence Detector (Applied Biosystems), according to the manufacturer's recommended conditions for real-time PCR, i.e., 1 cycle of 50°C for 2 minutes and 95°C for 10 minutes, followed by 30 cycles of 92°C for 15 seconds and 60°C for 60 seconds. Sequence-specific primers and probes were designed using Pre-Developed TaqMan Assay Reagents (Applied Biosystems). GAPDH was used to normalize messenger RNA (mRNA). Relative expression of real-time PCR products was determined using the $\Delta\Delta C_t$ method (12) to compare target gene and housekeeping gene mRNA expression. Each reaction was performed in triplicate.

T cell, B cell, macrophage, and neutrophil purification and stimulation. Splenocytes, bronchoalveolar lavage (BAL) fluid cells, and dermal draining (axillary) lymph node cells were obtained from 6–8-week-old untreated wild-type mice or mice with bleomycin-induced SSc, as previously described (11,23). T cells, B cells, macrophages, and neutrophils were enriched with respective isolation kits using an AutoMACS isolator (Miltenyi Biotec). More than 99% of these cells were CD3+, CD19+, F4/80+, and LY-6G+ (data not shown). Purified T cells, B cells, macrophages, and neutrophils (1×10^5) were cultured in RPMI 1640 containing 10% heat-inactivated fetal calf serum (Gibco Life Technologies). Cells were serum-starved for 12 hours and then stimulated for 10 hours with 100 ng/ml bleomycin with or without 10 μM edaravone, as described previously (24). To measure H_2O_2 and NO production, we used the cell-permeable probe dihydrorhodamine 123 (DHR-123) and diaminofluorescein (DAF-2DA), respectively as previously described (25,26). Cells were then subjected to flow cytometric analysis (FACScan; BD Biosciences). Each sample was tested in triplicate.

Fibroblast proliferation and collagen synthesis. Skin fibroblasts were obtained from 6–8-week-old untreated wild-type mice, mice with bleomycin-induced SSc, and TSK/+ mice, as described previously (27). Briefly, skin samples were obtained from the para-midline, lower back region of the mice. The purity of fibroblasts, as confirmed by flow cytometry, was >99%, with no leukocytes found in the harvested cells (data not shown). Cultured dermal fibroblasts (1.2×10^4/well) were seeded onto a 96-well plate. Fibroblasts were serum-starved for 12 hours and then cultured for 24 hours with graded concentrations of diethylamine NONOate (Cayman Chemicals), a long-acting NO-releasing agent, or H_2O_2 (Sigma), used as a hydroxyl radical–releasing agent, with or without 10 μM edaravone. NONOate and H_2O_2 were dissolved in PBS. The proliferation of cultured dermal fibroblasts was quantified using a colorimetric bromodeoxyuridine (BrdU) cell proliferation ELISA kit (Roche). After 24-hour incubation, BrdU (10 μM) was added to each well and incubated for 24 hours. To analyze the expression of mRNA for proα2(I) collagen (Col1a2), TGFβ1, and hyaluronan synthase 2 (HAS-2), total RNA was isolated from fibroblasts shortly after 24 hours of incubation with NONOate and H_2O_2. Each sample was tested in triplicate.

Statistical analysis. Data are expressed as the mean ± SD. The Mann-Whitney U test was used to determine the significance of differences between sample means, and analysis of variance followed by Bonferroni correction was used for multiple comparisons.

RESULTS

Attenuation by edaravone of bleomycin-induced skin and lung fibrosis. Previous studies have shown that skin fibrosis, lung fibrosis, and inflammatory cell infil-

tration develop during the first 4 weeks of bleomycin treatment, peak in the fourth week, and begin to resolve 6 weeks after the cessation of treatment (10,11). In the present study, skin fibrosis and lung fibrosis were histopathologically assessed 1, 2, 3, and 4 weeks after the initiation of bleomycin treatment in wild-type mice. Dermal thickness and lung fibrosis scores were increased in a time-dependent manner in bleomycin-treated mice (Figures 1A and B). After 2 weeks, dermal thickness in bleomycin-treated mice was significantly (1.4-fold) higher than that in PBS-treated mice ($P < 0.05$). Edaravone significantly reduced dermal fibrosis induced by bleomycin treatment ($P < 0.05$). After 4 weeks, edaravone had reduced dermal thickness in bleomycin-treated mice by 29% ($P < 0.01$) (Figures 1A and C). However, dermal thickness in mice treated with both bleomycin and edaravone remained greater than that in PBS-treated mice ($P < 0.01$). Dermal thickness was also assessed by quantifying the hydroxyproline content in 10-mg skin samples (Figure 1D). The hydroxyproline content in the skin of bleomycin-treated mice was increased by 2.1-fold over that in PBS-treated mice ($P < 0.01$); edaravone reduced the hydroxyproline content in the skin of bleomycin-treated mice by 26% ($P < 0.05$).

Similar results were obtained for the lung fibrosis score and pulmonary hydroxyproline content (Figures

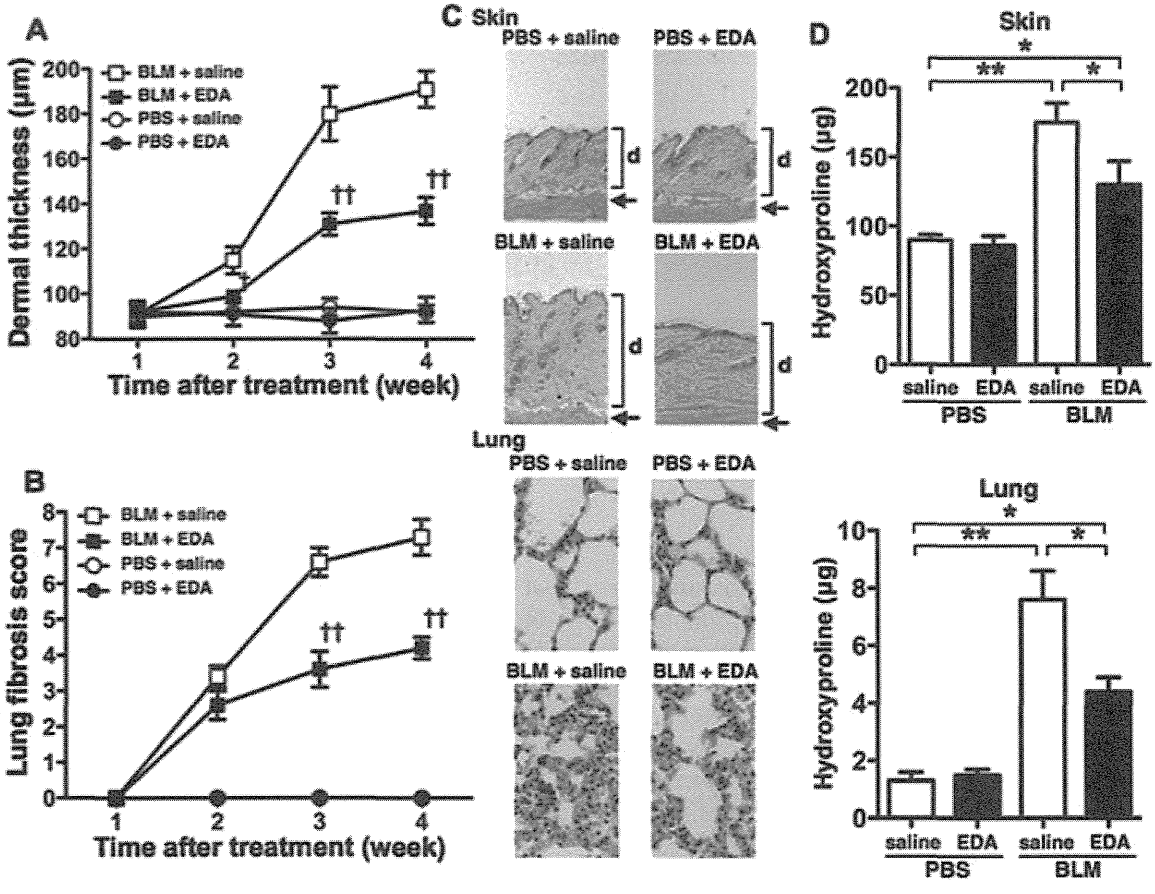

Figure 1. **A** and **B,** Dermal sclerosis (**A**) and lung fibrosis (**B**) in wild-type mice treated with phosphate buffered saline (PBS) or bleomycin (BLM) along with edaravone (EDA) or saline. Dermal and lung fibrosis was assessed by measuring dermal thickness and ascertaining the lung fibrosis score. **C,** Representative hematoxylin and eosin–stained histologic sections obtained after 4 weeks of treatment. d indicates dermis; **arrows** indicate panniculus carnosus. Original magnification × 100. **D,** Dermal and lung fibrosis assessed further by measurement of hydroxyproline content after 4 weeks of treatment. Values in **A, B,** and **D** are the mean ± SD results from 10 mice per group. † = $P < 0.05$; †† = $P < 0.01$, versus saline-treated mice with bleomycin-induced systemic sclerosis. * = $P < 0.05$; ** = $P < 0.01$.

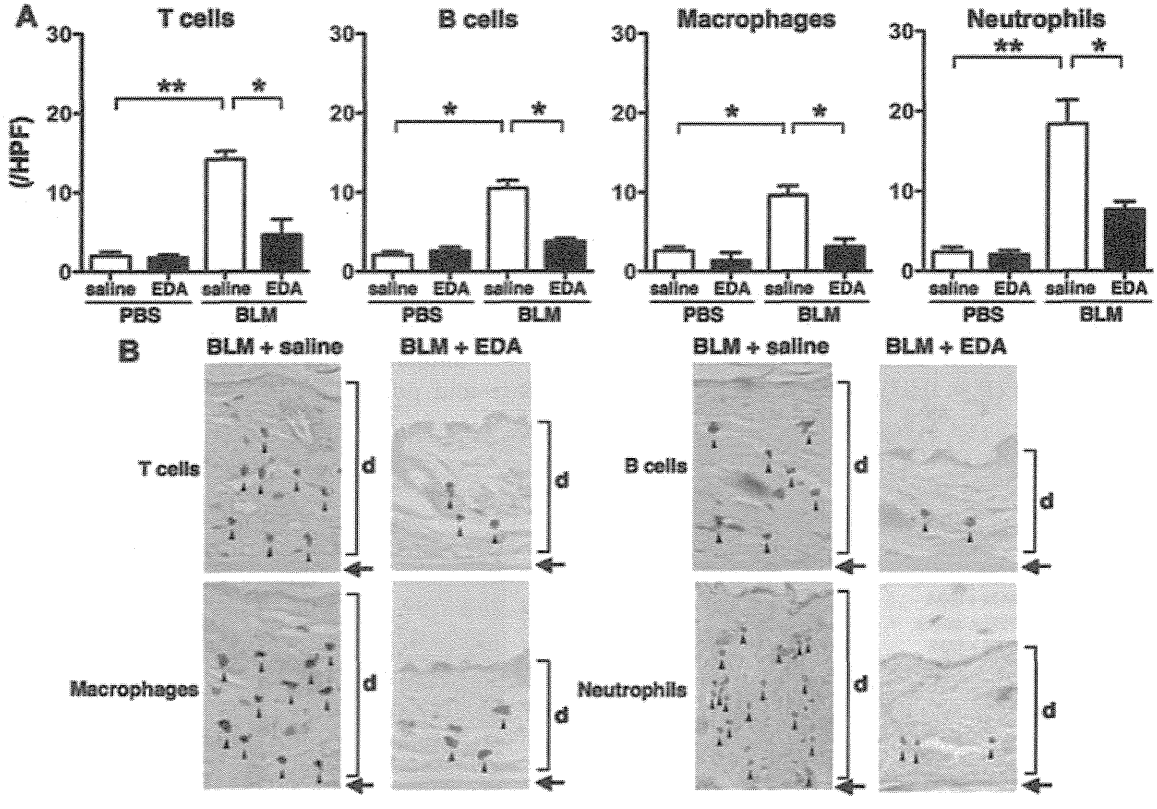

Figure 2. A, Numbers of T cells, B cells, macrophages, and neutrophils per high-power field (hpf) in wild-type mice treated with PBS or bleomycin along with edaravone or saline. Values are the mean ± SD results from 10 mice per group. * = $P <$ 0.05; ** = $P < 0.01$. **B,** Representative histologic sections. Neutrophils were identified by hematoxylin and eosin staining; T cells, B cells, and macrophages were stained with anti-CD3 monoclonal antibody (mAb), anti-B220 mAb, and anti-F4/80 mAb, respectively. d indicates dermis; **arrows** indicate panniculus carnosus. Original magnification × 200. See Figure 1 for other definitions.

1B–D). After 4 weeks, bleomycin-treated mice exhibited extensive inflammatory cell infiltration, fibrosis, alveolar injury, and increased hydroxyproline content. The histologic changes and hydroxyproline content were reduced by treatment with edaravone.

Inhibition by edaravone of inflammatory cell infiltration into skin. Numbers of immune cells in the skin of wild-type mice were assessed after 4 weeks of bleomycin treatment (Figure 2). The numbers of T cells, B cells, macrophages, and neutrophils in skin were greater in bleomycin-treated mice than in PBS-treated mice (all $P < 0.05$). Mice treated with both edaravone and bleomycin exhibited lower numbers of these cells compared with mice treated with bleomycin and saline (all $P < 0.05$). However, the numbers of neutrophils in mice treated with both edaravone and bleomycin remained significantly greater than in mice treated with PBS ($P < 0.05$).

Suppression by edaravone of the overproduction of cytokines, hyaluronan, H_2O_2, and NO in mice with bleomycin-induced SSc. We assessed the production of IL-6, TGFβ1, TNFα, IFNγ, hyaluronan, H_2O_2, and NO resulting from bleomycin injection (Figure 3). To measure NO production, we used a nitrite/nitrate assay, as described previously (28). Serum levels of cytokines, hyaluronan, H_2O_2, and nitrite/nitrate were elevated in bleomycin-treated wild-type mice compared with PBS-treated mice ($P < 0.01$). For each of these tested parameters except IFNγ, serum levels were reduced in mice treated with both edaravone and bleomycin compared with those in mice treated with bleomycin and saline ($P < 0.05$), but remained elevated compared with those in mice treated with PBS ($P < 0.05$) (Figure 3C). Like serum cytokine, hyaluronan, H_2O_2, and nitrite/nitrate levels, expression levels of mRNA for IL-6, TGFβ1, TNFα, and IFNγ in fibrotic skin and lung from

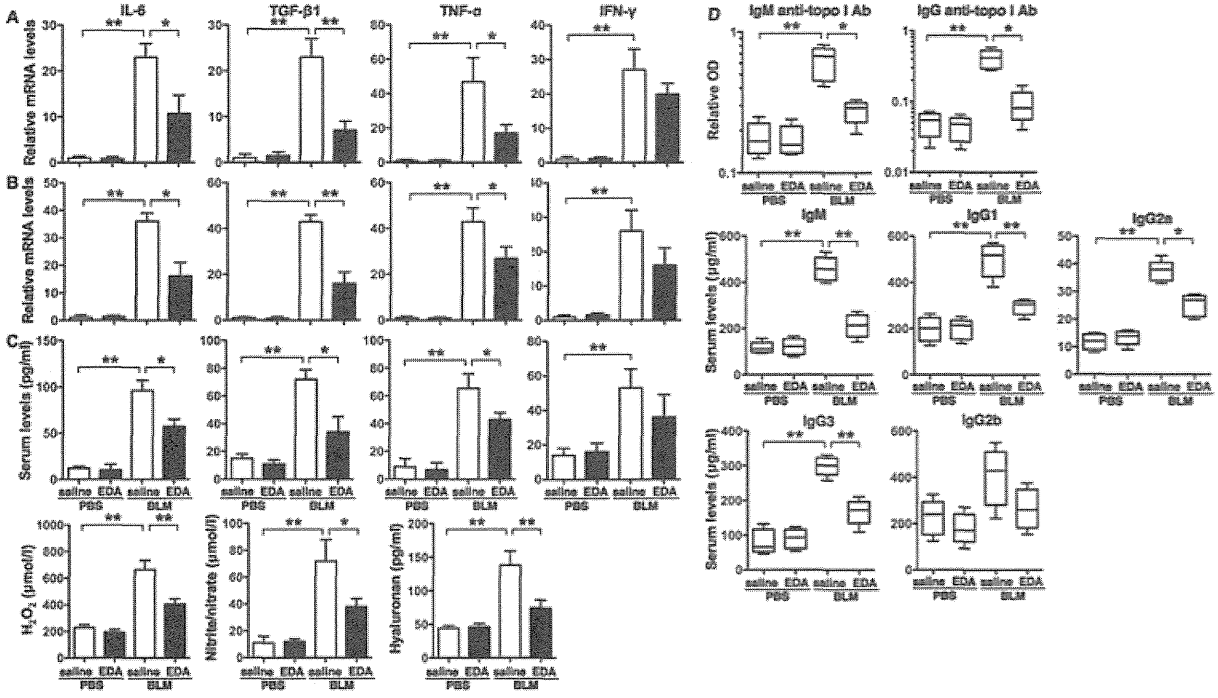

Figure 3. **A** and **B,** Expression of mRNA for interleukin-6 (IL-6), transforming growth factor $\beta 1$ (TGF$\beta 1$), tumor necrosis factor α (TNFα), and interferon-γ (IFNγ) in the skin (**A**) and lung (**B**) of wild-type (WT) mice treated with phosphate buffered saline (PBS) or bleomycin (BLM) along with edaravone (EDA) or saline. **C,** Protein levels of IL-6, TGF$\beta 1$, TNFα, and IFNγ and production of H_2O_2, nitric oxide (measured using a nitrite/nitrate assay), and hyaluronan in the serum of WT mice treated with PBS or bleomycin along with edaravone or saline. Values in **A–C** are the mean ± SD results from 10 mice per group. **D,** Serum levels of IgM and IgG anti–topoisomerase I antibody (anti–topo I Ab), IgM, and IgG subclasses in WT mice treated with PBS or bleomycin along with edaravone or saline. Data are presented as box plots, where the boxes represent the 25th to 75th percentiles, the lines within the boxes represent the median, and the lines outside the boxes represent the range of outlying values. * = $P < 0.05$; ** = $P < 0.01$. OD = optical density.

bleomycin-treated mice were higher than those in PBS-treated mice ($P < 0.01$) (Figures 3A and B), and edaravone inhibited the overproduction of mRNA for all of these cytokines ($P < 0.05$) except IFNγ.

Reduction by edaravone of bleomycin-induced autoantibody production. Bleomycin-treated mice produced significantly higher levels of anti–topo I antibody compared with PBS-treated mice ($P < 0.01$). However, anti–topo I levels in bleomycin-treated mice were reduced significantly by edaravone treatment ($P < 0.05$). Similarly, levels of IgM, IgG1, IgG2a, and IgG3 in bleomycin-treated mice were significantly elevated compared with levels in PBS-treated mice ($P < 0.01$), but edaravone treatment significantly reduced these Ig levels compared with saline treatment in bleomycin-treated mice ($P < 0.05$) (Figure 3D).

Reduction by edaravone of bleomycin-induced H_2O_2 and NO production by inflammatory cells. H_2O_2 and NO production in T cells, B cells, macrophages, and neutrophils from the spleens, skin draining lymph nodes, and BAL fluid of bleomycin-treated and PBS-treated mice was assessed by flow cytometry using the cell-permeable probe DHR-123 and DAF-2DA as previously described (25,26). With both DHR-123 and DAF-2DA, the mean fluorescence intensity (MFI) of B cells, macrophages, and neutrophils from bleomycin-treated mice was significantly higher than that of cells from PBS-treated mice (all $P < 0.01$), though the MFI of T cells obtained from bleomycin-treated mice was similar to that observed in T cells from PBS-treated mice (Figures 4A and B). In contrast, the MFI of B cells, macrophages, and neutrophils from mice treated with both edaravone and bleomycin was decreased compared with that in mice treated with bleomycin and saline ($P < 0.01$). However, the MFI values of these inflammatory cells from mice treated with edaravone and bleomycin remained significantly greater than those from PBS-treated mice ($P < 0.05$).

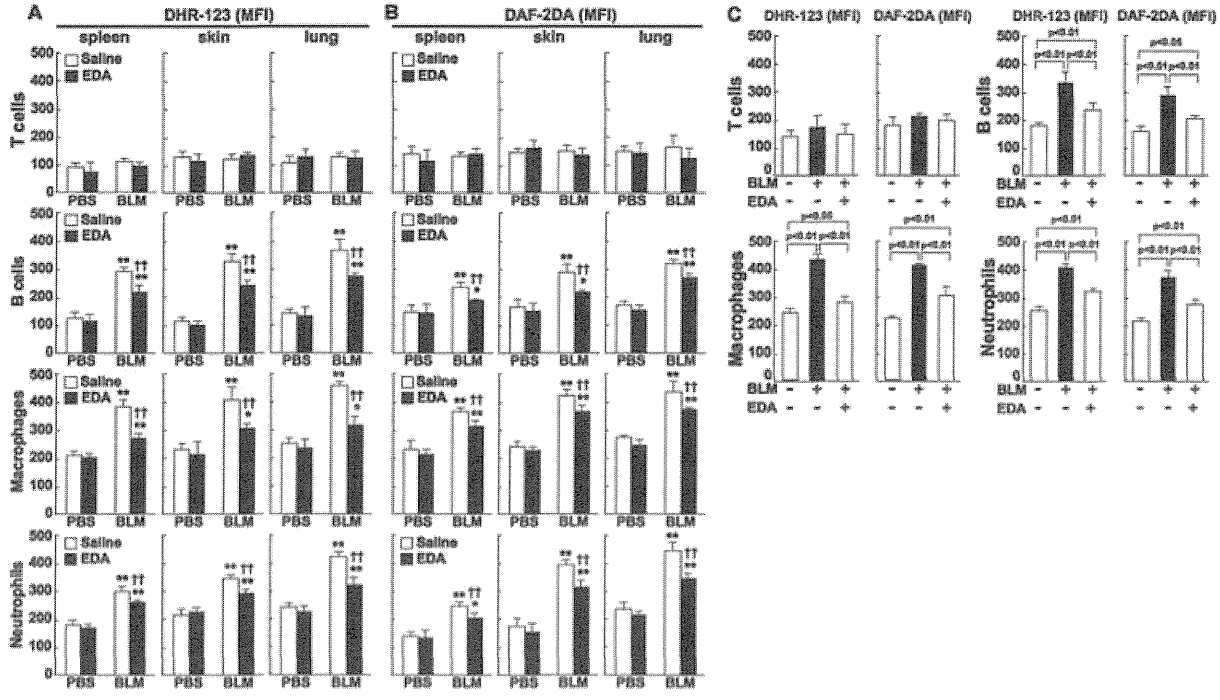

Figure 4. **A** and **B,** Production of H_2O_2 (**A**) and nitric oxide (NO) (**B**) in T cells, B cells, macrophages, and neutrophils of WT mice treated with PBS or bleomycin along with edaravone or saline. **C,** Production of H_2O_2 and NO in splenic T cells, B cells, macrophages, and neutrophils (purified from spleen, skin draining lymph nodes, and bronchoalveolar lavage fluid) from untreated WT mice after direct stimulation with 100 ng/ml bleomycin with or without 1 μM edaravone. H_2O_2 production and NO production were measured using the cell-permeable probe dihydrorhodamine 123 (DHR-123) and diaminofluorescein (DAF-2DA), respectively. Values are the mean ± SD mean fluorescence intensity (MFI) in 10 mice per group and are representative of 3 independent experiments. In **A** and **B,** $* = P < 0.05$; $** = P < 0.01$, versus the corresponding PBS-treated group. †† = $P < 0.01$ versus the bleomycin plus saline–treated group. See Figure 3 for other definitions.

Furthermore, we assessed H_2O_2 and NO production in T cells, B cells, macrophages, and neutrophils from the spleens of untreated wild-type mice after direct stimulation with bleomycin in various concentrations. In experiments using DHR-123 and DAF-2DA, treatment with 100 ng/ml bleomycin yielded the highest MFI values in B cells, macrophages, and neutrophils ($P < 0.01$), whereas bleomycin did not affect the MFI in T cells (Figure 4C). MFI values obtained with DHR-123 and DAF-2DA were significantly reduced by treatment with both edaravone and bleomycin compared to those observed with treatment with bleomycin only ($P < 0.01$).

Attenuation by edaravone of the development of skin fibrosis and production of cytokines, hyaluronan, autoantibodies, H_2O_2, and NO in TSK/+ mice. Skin fibrosis in TSK/+ mice treated with edaravone or saline was assessed histopathologically at 1, 2, 3, and 4 weeks after the initiation of treatment (Figure 5A). Hypodermal thickness was also assessed by quantifying the hydroxyproline content of 10-mg skin samples from TSK/+ and wild-type mice (Figure 5A). Both hypodermal thickness and hydroxyproline content increased in a time-dependent manner in TSK/+ mice. After 4 weeks, hypodermal thickness and hydroxyproline content were significantly lower in edaravone-treated TSK/+ mice than in saline-treated TSK/+ mice ($P < 0.01$ and $P < 0.05$, respectively).

Similarly, although levels of mRNA for IL-6 and TGFβ1 were increased in the skin of saline-treated TSK/+ mice compared to saline-treated wild-type mice ($P < 0.01$), edaravone-treated TSK/+ mice exhibited lower levels of IL-6 and TGFβ1 mRNA than were observed in saline-treated TSK/+ mice ($P < 0.05$) (Figure 5B). Edaravone did not affect the levels of mRNA for TNFα or IFNγ.

Furthermore, saline-treated TSK/+ mice showed higher serum levels of anti–topo I antibody ($P < 0.05$) (Figure 5C) and production of hyaluronan, H_2O_2, and nitrite/nitrate ($P < 0.01$) (Figure 5D) compared with saline-treated wild-type mice. Edaravone treatment sig-

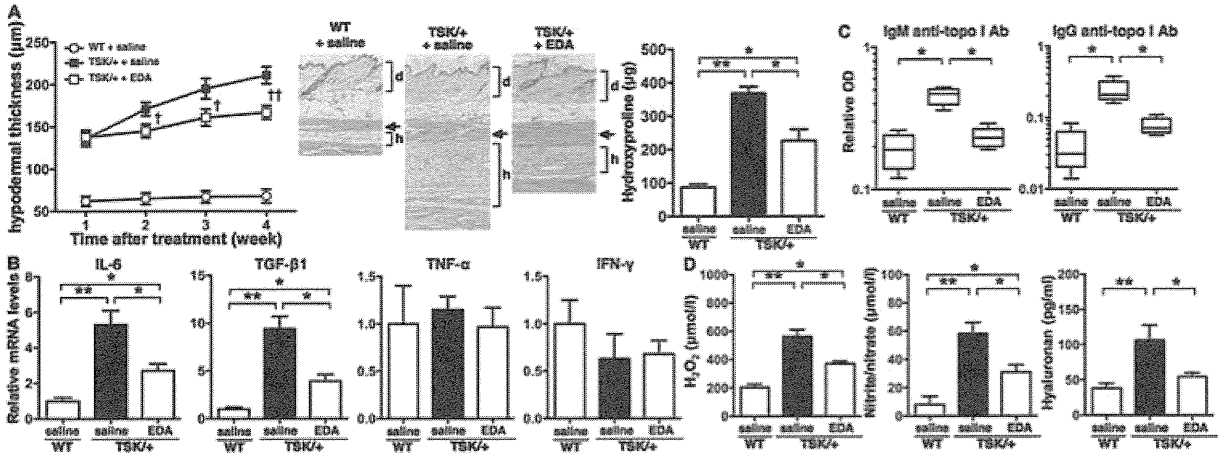

Figure 5. A, Hypodermal fibrosis in the dorsal skin of TSK/+ mice treated with edaravone or saline and WT littermates treated with saline. Hypodermal fibrosis was assessed by measuring hypodermal thickness 1, 2, 3, and 4 weeks after treatment (left) and by determining skin hydroxyproline content 4 weeks after treatment (right). † = $P < 0.05$; †† = $P < 0.01$, versus saline-treated TSK/+ mice. Representative hematoxylin and eosin–stained histologic sections obtained after 4 weeks of treatment are also shown (center). d indicates dermis; h indicates hypodermis; **arrows** indicate panniculus carnosus. Original magnification × 100. **B–D,** Expression of mRNA for IL-6, TGFβ1, TNFα, and IFNγ in the skin (**B**) and levels of anti–topo I antibody (**C**) and production of H_2O_2, nitric oxide (measured using a nitrite/nitrate assay), and hyaluronan (**D**) in the serum of TSK/+ mice treated with edaravone or saline and WT littermates treated with saline. Values in **A, B,** and **D** are the mean ± SD results from 10 mice per group. Data in **C** are presented as box plots, where the boxes represent the 25th to 75th percentiles, the lines within the boxes represent the median, and the lines outside the boxes represent the range of outlying values. * = $P < 0.05$; ** = $P < 0.01$. See Figure 3 for definitions.

nificantly reduced these elevations ($P < 0.05$). There was no significant difference in hypodermal thickness, hydroxyproline content, or cytokine, hyaluronan, autoantibody, H_2O_2, or nitrite/nitrate production between edaravone-treated and saline-treated wild-type mice (data not shown).

Suppression by edaravone of NONOate- or H_2O_2-induced Col1a2, TGFβ1, and HAS-2 mRNA overexpression in fibroblasts. To assess the responsiveness of fibroblasts to free radicals, we stimulated wild-type mouse fibroblasts with various concentrations of NONOate, an NO donor, or H_2O_2 (Figure 6A). NONOate and H_2O_2 increased expression of mRNA for Col1a2, TGFβ1, and HAS-2 in a dose-dependent manner; Col1a2, TGFβ1, and HAS-2 mRNA expression was increased most strongly with NONOate at 200 μg/ml or H_2O_2 at 1 mmole/liter ($P < 0.01$). Edaravone treatment significantly reduced the mRNA overexpression ($P < 0.01$). However, NONOate and H_2O_2 did not affect proliferation in wild-type mouse fibroblasts. Similar results were obtained using fibroblasts from bleomycin-treated wild-type mice and from TSK/+ mice (Figures 6B and C). In addition, stimulation with 200 μg/ml NONOate or 1 mmole/liter H_2O_2 induced significantly greater Col1a2, TGFβ1, and HAS-2 mRNA expression in fibroblasts from bleomycin-treated wild-type mice and TSK/+ mice than in fibroblasts from untreated wild-type mice ($P < 0.01$) (Figures 6B and C). Treatment with edaravone attenuated this mRNA overexpression ($P < 0.01$), but expression levels remained higher in fibroblasts from bleomycin-treated wild-type mice and TSK/+ mice than in fibroblasts from untreated wild-type mice ($P < 0.05$).

DISCUSSION

Edaravone is a free radical scavenger that has been approved as a therapeutic agent for acute cerebral infarction (17,18). It was recently shown that edaravone reduced lung fibrosis in mice with intratracheal bleomycin–induced lung fibrosis (19,29,30). However, to date there has been no published study on the effect of edaravone on fibrosis in mice with experimental SSc. The present study is the first to demonstrate that edaravone inhibits the development of dermal and lung fibrosis, inflammatory cell infiltration, hypergammaglobulinemia, and autoantibody production induced by bleomycin (Figures 1, 2, and 3D). In addition, edaravone suppressed the production of various cytokines, including fibrogenic IL-6, TGFβ1, and TNFα, in the skin of bleomycin-treated mice (Figures 3A–C). Furthermore, edaravone reduced hypodermal thickening, cytokine

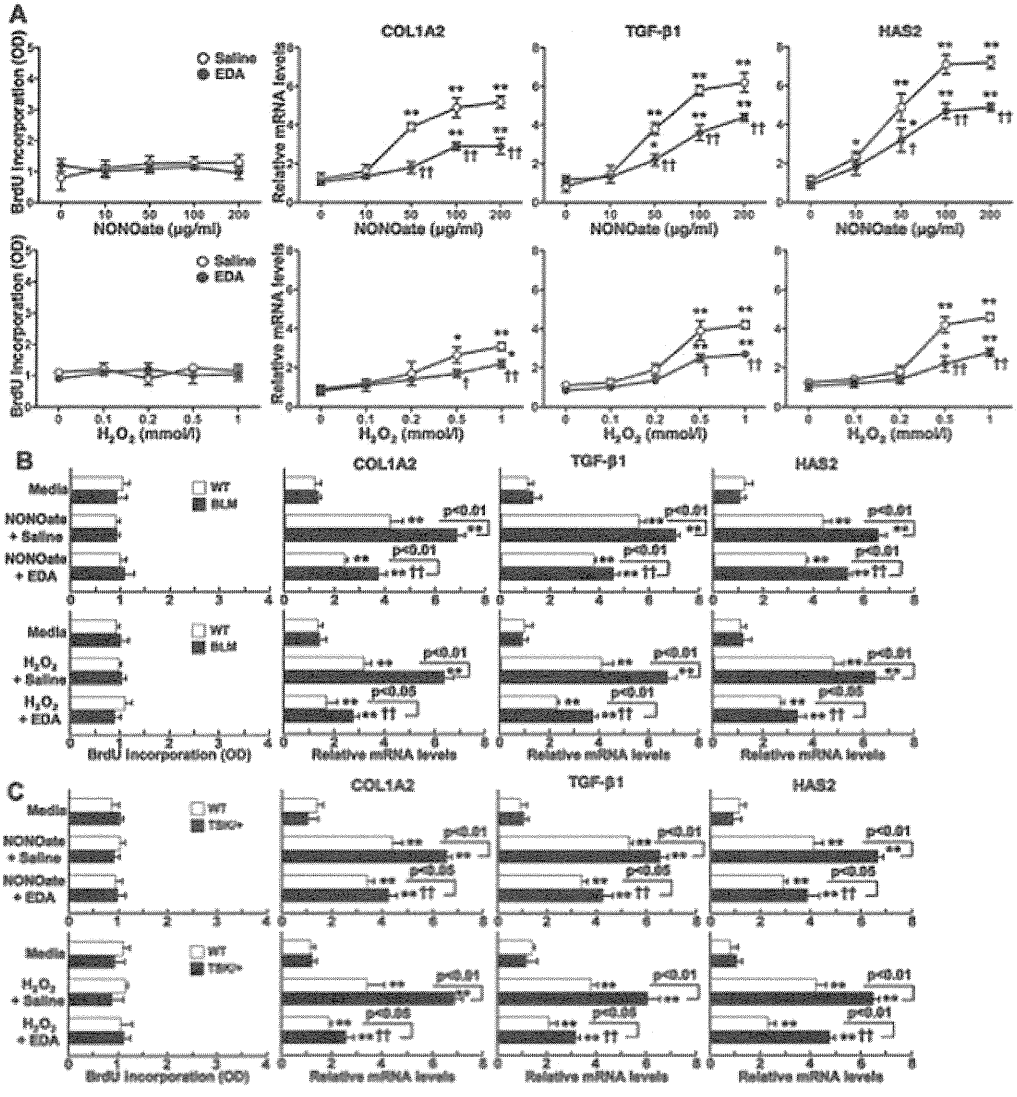

Figure 6. Proliferation of and proα2(I) collagen (Col1a2), TGFβ1, and hyaluronan synthase 2 (HAS-2) mRNA expression in dermal fibroblasts from untreated WT mice, bleomycin-treated WT mice, and TSK/+ mice. **A,** After 24 hours of stimulation with NONOate and H_2O_2 in various concentrations with or without 10 μM edaravone, total RNA from fibroblasts of untreated WT mice was extracted, and expression of Col1a2, TGFβ1, and HAS-2 mRNA was analyzed by real-time polymerase chain reaction and normalized to the internal control GAPDH. Bromodeoxyuridine (BrdU) incorporation in proliferating cells was quantified by enzyme-linked immunosorbent assay. Values are the mean ± SD results from 10 mice per group. $*$ = $P < 0.05$; $**$ = $P < 0.01$, versus the pretreatment value. † = $P < 0.05$; †† = $P < 0.01$, versus the corresponding saline-treated group. **B** and **C,** Fibroblasts from bleomycin-treated WT mice (**B**) and TSK/+ mice (**C**) were stimulated with 200 μg/ml NONOate and 1 mmole/liter of H_2O_2 with or without 10 μM edaravone, and expression of Col1a2, TGFβ1, and HAS-2 mRNA was measured. Values are the mean ± SD results from 10 mice per group. $*$ = $P < 0.05$; $**$ = $P < 0.01$, versus the corresponding media-treated group. † = $P < 0.05$; †† = $P < 0.01$, versus the corresponding saline-treated group. See Figure 3 for other definitions.

production, and autoantibody production in TSK/+ mice (Figure 5). Collectively, these results suggest that edaravone ameliorates fibrosis by reducing oxidative stress both in mice with bleomycin-induced SSc and in TSK/+ mice.

Recent studies have shown that bleomycin treat-

ment induces oxidative stress, which in turn induces up-regulation of fibrogenic cytokine production, collagen synthesis, and inflammatory cell infiltration (11,19, 31,32). Indeed, in the present study bleomycin-treated mice exhibited elevated levels of H_2O_2 and NO (Figure 3C). Moreover, oxidative stress can directly induce collagen production from fibroblasts (33–36), and in this study stimulation with NONOate, a long-acting NO-releasing agent, and H_2O_2 increased collagen and TGFβ1 expression in fibroblasts (Figure 6). In addition, bleomycin itself directly stimulates inflammatory cells (11,37). Previous studies indicate that free radical production is increased in stimulated immune cells (38–40), and in the present study, bleomycin enhanced H_2O_2 and NO production by B cells, macrophages, and neutrophils (Figure 4). Similar to findings in mice with bleomycin-induced SSc, oxidative stress plays important roles in fibrosis in TSK/+ mice (16,41). TSK/+ mice exhibit endothelial dysfunction, which results in increased free radical production (42). In the present study, serum levels of H_2O_2 and NO were increased in these mice (Figure 5D). Thus, these results suggest that edaravone inhibits oxidative stress–dependent cytokine and collagen production, which results in reduction of fibrosis in both mice with bleomycin-induced SSc and TSK/+ mice.

Abnormal activation of immune cells, including T cells, B cells, macrophages, and neutrophils, has been identified in SSc (43). Furthermore, activated immune cell infiltration was found in the sclerotic skin and fibrotic lung (44), indicating that immune activation leads to fibrosis through stimulation of collagen production by fibroblasts. These immune cells also infiltrate the fibrotic skin and lung of mice with bleomycin-induced SSc and the sclerotic skin of TSK/+ mice (11,12,27). In this study, bleomycin induced inflammatory cell infiltration, which was reduced by edaravone treatment (Figure 2). Moreover, edaravone treatment reduced autoimmune reactions in mice with bleomycin-induced SSc and TSK/+ mice (Figures 3D and 5C).

Previous investigations have revealed an important role of endogenous ligands for TLR, such as hyaluronan, in the development of autoimmune diseases (45). The endogenous TLR ligands induce inflammatory cell activation and infiltration and are associated with the severity of autoimmune diseases. In SSc patients, serum levels of hyaluronan and high mobility group box chromosomal protein 1, another endogenous ligand for TLR, are increased and correlate with skin sclerosis, lung fibrosis, and autoimmune abnormalities (46,47). Indeed, in this study we observed increased serum levels of hyaluronan in mice with bleomycin-induced SSc and TSK/+ mice (Figures 3C and 5D). Earlier studies indicate that hyaluronan synthesis is regulated by 3 synthases, HAS-1, HAS-2, and HAS3 (48). HAS-2 expression, in particular, is up-regulated by oxidative stress (49). In the present investigation, HAS-2 expression was increased in fibroblasts stimulated with free radical–releasing agents (Figure 6). Thus, enhanced free radical production, which is a common feature of human SSc, may play a role as an initiator of immunologic abnormalities via overproduction of endogenous TLR ligands. Taken together, these results suggest that edaravone abrogates fibrosis by reducing inflammatory cell activation both in mice with bleomycin-induced SSc and in TSK/+ mice.

This study is the first to demonstrate that edaravone has significant inhibitory effects on fibrosis in both mice with bleomycin-induced SSc and TSK/+ mice. Edaravone is already used in the treatment of embolic stroke and is being evaluated in clinical trials of amyotrophic lateral sclerosis. Since current therapies for the skin and lung fibrosis of SSc are at present insufficient, the present results suggest that edaravone warrants evaluation as a novel antifibrotic agent.

ACKNOWLEDGMENTS

We thank Mariko Yozaki, Aya Usui, and Kaori Shimoda for technical assistance.

AUTHOR CONTRIBUTIONS

All authors were involved in drafting the article or revising it critically for important intellectual content, and all authors approved the final version to be published. Dr. Sato had full access to all of the data in the study and takes responsibility for the integrity of the data and the accuracy of the data analysis.

Study conception and design. Yoshizaki, Sato.

Acquisition of data. Yoshizaki, Yanaba, A. Ogawa, Iwata, F. Ogawa.

Analysis and interpretation of data. Yoshizaki, A. Ogawa, Takenaka, Shimizu, Asano, Kadono, Sato.

REFERENCES

1. LeRoy EC, Black C, Fleischmajer R, Jablonska S, Krieg T, Medsger TA Jr, et al. Scleroderma (systemic sclerosis): classification, subsets and pathogenesis. J Rheumatol 1988;15:202–5.
2. Jinnin M. Mechanisms of skin fibrosis in systemic sclerosis. J Dermatol 2010;37:11–25.
3. Okano Y. Antinuclear antibody in systemic sclerosis (scleroderma). Rheum Dis Clin North Am 1996;22:709–35.
4. Sambo P, Baroni SS, Luchetti M, Paroncini P, Dusi S, Orlandini G, et al. Oxidative stress in scleroderma: maintenance of scleroderma fibroblast phenotype by the constitutive up-regulation of reactive oxygen species generation through the NADPH oxidase complex pathway. Arthritis Rheum 2001;44:2653–64.

5. Ogawa F, Shimizu K, Muroi E, Hara T, Hasegawa M, Takehara K, et al. Serum levels of 8-isoprostane, a marker of oxidative stress, are elevated in patients with systemic sclerosis. Rheumatology (Oxford) 2006;45:815–8.
6. Simonini G, Pignone A, Generini S, Falcini F, Cerinic MM. Emerging potentials for an antioxidant therapy as a new approach to the treatment of systemic sclerosis. Toxicology 2000;155:1–15.
7. Abraham D, Distler O. How does endothelial cell injury start? The role of endothelin in systemic sclerosis. Arthritis Res Ther 2007;9 Suppl 2:S2.
8. Servettaz A, Goulvestre C, Kavian N, Nicco C, Guilpain P, Chereau C, et al. Selective oxidation of DNA topoisomerase 1 induces systemic sclerosis in the mouse. J Immunol 2009;182: 5855–64.
9. Campo GM, Avenoso A, Campo S, D'Ascola A, Traina P, Sama D, et al. The antioxidant effect exerted by TGF-1β-stimulated hyaluronan production reduced NF-κB activation and apoptosis in human fibroblasts exposed to FeSo4 plus ascorbate. Mol Cell Biochem 2008;311:167–77.
10. Yamamoto T. The bleomycin-induced scleroderma model: what have we learned for scleroderma pathogenesis? Arch Dermatol Res 2006;297:333–44.
11. Yoshizaki A, Iwata Y, Komura K, Ogawa F, Hara T, Muroi E, et al. CD19 regulates skin and lung fibrosis via Toll-like receptor signaling in a model of bleomycin-induced scleroderma. Am J Pathol 2008;172:1650–63.
12. Yoshizaki A, Yanaba K, Yoshizaki A, Iwata Y, Komura K, Ogawa F, et al. Treatment with rapamycin prevents fibrosis in tight-skin and bleomycin-induced mouse models of systemic sclerosis. Arthritis Rheum 2010;62:2476–87.
13. Akhmetshina A, Venalis P, Dees C, Busch N, Zwerina J, Schett G, et al. Treatment with imatinib prevents fibrosis in different preclinical models of systemic sclerosis and induces regression of established fibrosis. Arthritis Rheum 2009;60:219–24.
14. Inghilleri S, Morbini P, Oggionni T, Barni S, Fenoglio C. In situ assessment of oxidant and nitrogenic stress in bleomycin pulmonary fibrosis. Histochem Cell Biol 2006;125:661–9.
15. Manoury B, Nenan S, Leclerc O, Guenon I, Boichot E, Planquois JM, et al. The absence of reactive oxygen species production protects mice against bleomycin-induced pulmonary fibrosis. Respir Res 2005;6:11.
16. Dooley A, Low SY, Holmes A, Kidane AG, Abraham DJ, Black CM, et al. Nitric oxide synthase expression and activity in the tight-skin mouse model of fibrosis. Rheumatology (Oxford) 2008; 47:272–80.
17. Edaravone Acute Infarction Study Group. Effect of a novel free radical scavenger, edaravone (MCI-186), on acute brain infarction: randomized, placebo-controlled, double-blind study at multicenters. Cerebrovasc Dis 2003;15:222–9.
18. Yoshida H, Yanai H, Namiki Y, Fukatsu-Sasaki K, Furutani N, Tada N. Neuroprotective effects of edaravone: a novel free radical scavenger in cerebrovascular injury. CNS Drug Rev 2006;12:9–20.
19. Asai T, Ohno Y, Minatoguchi S, Funaguchi N, Yuhgetsu H, Sawada M, et al. The specific free radical scavenger edaravone suppresses bleomycin-induced acute pulmonary injury in rabbits. Clin Exp Pharmacol Physiol 2007;34:22–6.
20. Zhang N, Komine-Kobayashi M, Tanaka R, Liu M, Mizuno Y, Urabe T. Edaravone reduces early accumulation of oxidative products and sequential inflammatory responses after transient focal ischemia in mice brain. Stroke 2005;36:2220–5.
21. Hishida A. Clinical analysis of 207 patients who developed renal disorders during or after treatment with edaravone reported during post-marketing surveillance. Clin Exp Nephrol 2007;11: 292–6.
22. Ashcroft T, Simpson JM, Timbrell V. Simple method of estimating severity of pulmonary fibrosis on a numerical scale. J Clin Pathol 1988;41:467–70.
23. Byrne SN, Limon-Flores AY, Ullrich SE. Mast cell migration from the skin to the draining lymph nodes upon ultraviolet irradiation represents a key step in the induction of immune suppression. J Immunol 2008;180:4648–55.
24. Kawasaki T, Kitao T, Nakagawa K, Fujisaki H, Takegawa Y, Koda K, et al. Nitric oxide-induced apoptosis in cultured rat astrocytes: protection by edaravone, a radical scavenger. Glia 2007;55:1325–33.
25. Lacy P, Abdel-Latif D, Steward M, Musat-Marcu S, Man SF, Moqbel R. Divergence of mechanisms regulating respiratory burst in blood and sputum eosinophils and neutrophils from atopic subjects. J Immunol 2003;170:2670–9.
26. Schnyder B, Pittet M, Durand J, Schnyder-Candrian S. Rapid effects of glucose on the insulin signaling of endothelial NO generation and epithelial Na transport. Am J Physiol Endocrinol Metab 2002;282:E87–94.
27. Yoshizaki A, Yanaba K, Iwata Y, Komura K, Ogawa A, Akiyama Y, et al. Cell adhesion molecules regulate fibrotic process via Th1/Th2/Th17 cell balance in a bleomycin-induced scleroderma model. J Immunol 2010;185:2502–15.
28. Ding J, Song D, Ye X, Liu SF. A pivotal role of endothelial-specific NF-κB signaling in the pathogenesis of septic shock and septic vascular dysfunction. J Immunol 2009;183:4031–8.
29. Fujita M, Mizuta Y, Ikegame S, Ouchi H, Ye Q, Harada E, et al. Biphasic effects of free radical scavengers against bleomycin-induced pulmonary fibrosis. Pulm Pharmacol Ther 2008;21: 805–11.
30. Tajima S, Bando M, Ishii Y, Hosono T, Yamasawa H, Ohno S, et al. Effects of edaravone, a free-radical scavenger, on bleomycin-induced lung injury in mice. Eur Respir J 2008;32:1337–43.
31. Jeannin P, Delneste Y, Lecoanet-Henchoz S, Gauchat JF, Life P, Holmes D, et al. Thiols decrease human interleukin (IL) 4 production and IL-4-induced immunoglobulin synthesis. J Exp Med 1995;182:1785–92.
32. Peterson JD, Herzenberg LA, Vasquez K, Waltenbaugh C. Glutathione levels in antigen-presenting cells modulate Th1 versus Th2 response patterns. Proc Natl Acad Sci U S A 1998;95:3071–6.
33. Falanga V, Martin TA, Takagi H, Kirsner RS, Helfman T, Pardes J, et al. Low oxygen tension increases mRNA levels of α1 (I) procollagen in human dermal fibroblasts. J Cell Physiol 1993;157: 408–12.
34. Parola M, Pinzani M, Casini A, Albano E, Poli G, Gentilini A, et al. Stimulation of lipid peroxidation or 4-hydroxynonenal treatment increases procollagen α1 (I) gene expression in human liver fat-storing cells. Biochem Biophys Res Commun 1993;194: 1044–50.
35. Bellocq A, Azoulay E, Marullo S, Flahault A, Fouqueray B, Philippe C, et al. Reactive oxygen and nitrogen intermediates increase transforming growth factor-β1 release from human epithelial alveolar cells through two different mechanisms. Am J Respir Cell Mol Biol 1999;21:128–36.
36. Gabrielli A, Svegliati S, Moroncini G, Pomponio G, Santillo M, Avvedimento EV. Oxidative stress and the pathogenesis of scleroderma: the Murrell's hypothesis revisited. Semin Immunopathol 2008;30:329–37.
37. Jiang D, Liang J, Fan J, Yu S, Chen S, Luo Y, et al. Regulation of lung injury and repair by Toll-like receptors and hyaluronan. Nat Med 2005;11:1173–9.
38. Ding AH, Nathan CF, Stuehr DJ. Release of reactive nitrogen intermediates and reactive oxygen intermediates from mouse peritoneal macrophages: comparison of activating cytokines and evidence for independent production. J Immunol 1988;141: 2407–12.
39. Iharada A, Kaneko K, Tsuji S, Hasui M, Kanda S, Nishiyama T. Increased nitric oxide production by T- and B-cells in idiopathic nephrotic syndrome. Pediatr Nephrol 2009;24:1033–8.
40. Kobayashi S, Imajoh-Ohmi S, Kuribayashi F, Nunoi H, Nakamura

M, Kanegasaki S. Characterization of the superoxide-generating system in human peripheral lymphocytes and lymphoid cell lines. J Biochem 1995;117:758–65.
41. Weihrauch D, Xu H, Shi Y, Wang J, Brien J, Jones DW, et al. Effects of D-4F on vasodilation, oxidative stress, angiostatin, myocardial inflammation, and angiogenic potential in tight-skin mice. Am J Physiol Heart Circ Physiol 2007;293:H1432–41.
42. Marie I, Beny JL. Endothelial dysfunction in murine model of systemic sclerosis: tight-skin mice 1. J Invest Dermatol 2002;119: 1379–87.
43. Sato S, Fujimoto M, Hasegawa M, Takehara K. Altered blood B lymphocyte homeostasis in systemic sclerosis: expanded naive B cells and diminished but activated memory B cells. Arthritis Rheum 2004;50:1918–27.
44. Tashkin DP, Elashoff R, Clements PJ, Goldin J, Roth MD, Furst DE, et al. Cyclophosphamide versus placebo in scleroderma lung disease. N Engl J Med 2006;354:2655–66.
45. Marshak-Rothstein A. Toll-like receptors in systemic autoimmune disease. Nat Rev Immunol 2006;6:823–35.
46. Yoshizaki A, Komura K, Iwata Y, Ogawa F, Hara T, Muroi E, et al. Clinical significance of serum HMGB-1 and sRAGE levels in systemic sclerosis: association with disease severity. J Clin Immunol 2009;29:180–9.
47. Yoshizaki A, Iwata Y, Komura K, Hara T, Ogawa F, Muroi E, et al. Clinical significance of serum hyaluronan levels in systemic sclerosis: association with disease severity. J Rheumatol 2008;35: 1825–9.
48. Itano N, Kimata K. Mammalian hyaluronan synthases. IUBMB Life 2002;54:195–9.
49. Campo GM, Avenoso A, Campo S, Angela D, Ferlazzo AM, Calatroni A. TNF-α, IFN-γ, and IL-1β modulate hyaluronan synthase expression in human skin fibroblasts: synergistic effect by concomital treatment with FeSO4 plus ascorbate. Mol Cell Biochem 2006;292:169–78.

ARTHRITIS & RHEUMATISM
Vol. 63, No. 11, November 2011, pp 3575–3585
DOI 10.1002/art.30539

Immunization With DNA Topoisomerase I and Freund's Complete Adjuvant Induces Skin and Lung Fibrosis and Autoimmunity via Interleukin-6 Signaling

Ayumi Yoshizaki,[1] Koichi Yanaba,[1] Asako Ogawa,[1] Yoshihide Asano,[2] Takafumi Kadono,[2] and Shinichi Sato[2]

Objective. **The presence of anti–DNA topoisomerase I (anti–topo I) antibody correlates positively with disease severity in patients with systemic sclerosis (SSc). However, the role of induction of anti–topo I antibody production and its potential contribution to the pathogenesis of SSc remain unclear. The aim of this study was to examine the role of anti–topo I antibody in the pathogenesis of SSc.**

Methods. **To assess the contribution of anti–topo I antibody to the pathogenetic process, dermal sclerosis, pulmonary fibrosis, and cytokine production were examined in mice treated with topo I and either Freund's complete adjuvant (CFA) or Freund's incomplete adjuvant (IFA).**

Results. **Treatment with topo I and CFA, in contrast to treatment with topo I and IFA, induced skin and lung fibrosis with increased interleukin-6 (IL-6), transforming growth factor β1, and IL-17 production and decreased IL-10 production. Anti–topo I antibody levels were greater in mice treated with topo I and CFA than in mice treated with topo I and IFA. Furthermore, treatment with topo I and CFA increased Th2 and Th17 cell frequencies in bronchoalveolar lavage fluid, whereas treatment with topo I and IFA increased Th1 and Treg cell frequencies. Moreover, loss of IL-6 expression ameliorated skin and lung fibrosis, decreased Th2 and Th17 cell frequencies, and increased Th1 and Treg cell frequencies.**

Conclusion. **This study is the first to show that treatment with topo I and CFA induces SSc-like skin and lung fibrosis and autoimmune abnormalities. We also suggest that IL-6 plays important roles in the development of fibrosis and autoimmune abnormalities in this novel SSc model.**

Systemic sclerosis (SSc) is a connective tissue disease characterized by excessive extracellular matrix deposition with an autoimmune background (1). The presence of autoantibodies is a central feature of SSc, since antinuclear antibodies (ANAs), such as anti–DNA topoisomerase I (anti–topo I) antibody, are detected in >90% of patients (2). Furthermore, abnormal activation of several immune cells has been identified in SSc (3). A recent study has shown that skin and lung fibrosis is ameliorated by treatment with cyclophosphamide, an immunosuppressive agent, indicating that immune activation leads to fibrosis through the stimulation of collagen production by fibroblasts (4). Indeed, SSc patients exhibit infiltration of inflammatory cells, especially CD4+ T cells, and elevated serum levels of various cytokines, especially fibrogenic Th2 and Th17 cytokines and transforming growth factor β1 (TGFβ1), a major fibrogenic growth factor, which correlate positively with disease severity (5,6).

Autoimmune responses with high levels of circulating autoantibodies are commonly detected in patients with rheumatic diseases (7). Furthermore, specific autoantibodies are associated with clinical subsets of a particular autoimmune disease. Anti–topo I antibody is detected more frequently in SSc patients with diffuse cutaneous thickening than in those with limited cutane-

Supported by the Ministry of Health, Labor, and Welfare of Japan (Research on Intractable Diseases grant to Drs. Yoshizaki and Sato).

[1]Ayumi Yoshizaki, MD, PhD, Koichi Yanaba, MD, PhD, Asako Ogawa, MD: Nagasaki University Graduate School of Biomedical Sciences, Nagasaki, Japan; [2]Yoshihide Asano, MD, PhD, Takafumi Kadono, MD, PhD, Shinichi Sato, MD, PhD: University of Tokyo Graduate School of Medicine, Tokyo, Japan.

Address correspondence to Shinichi Sato, MD, PhD, Department of Dermatology, University of Tokyo Graduate School of Medicine, 7-3-1 Hongo, Bunkyo-ku, Tokyo 113-8655, Japan. E-mail: satos-der@h.u-tokyo.ac.jp.

Submitted for publication November 12, 2010; accepted in revised form June 30, 2011.

ous thickening (8). The presence of anti–topo I antibody correlates positively with dermal sclerosis, pulmonary fibrosis, and overproduction of inflammatory cytokines (9–11). These data indicate that serum levels of anti–topo I antibody are associated with disease severity and/or activity in patients with SSc. In addition, anti–topo I antibodies have been detected in mouse models of SSc (12,13). These studies strongly suggest a close relationship of autoimmune responses to the pathogenesis of SSc. However, the role of induction of anti–topo I antibody production and its potential contribution to the pathogenesis of SSc remain unclear.

A recent study indicated that mice immunized with recombinant human topo I protein emulsified in Freund's complete adjuvant (CFA) and boosted with topo I emulsified in Freund's incomplete adjuvant (IFA) showed anti–topo I antibody production (14). However, these mice did not show dermal and pulmonary fibrosis (14). Previously, in an experimental autoimmune encephalomyelitis (EAE) model, treatment with myelin oligodendrocyte glycoprotein (MOG) and IFA, in contrast to treatment with MOG and CFA, did not induce interleukin-6 (IL-6) production (15). In the absence of IL-6, Th17 cell responses are impaired whereas Treg cell responses are dominant, suggesting that IL-6 is a critical factor that shifts the immune response from Treg cell responses toward pathogenic Th17 cell responses (16,17). Indeed, in contrast to treatment with MOG and CFA, treatment with MOG and IFA did not trigger antigen-specific production of IL-17 (15). Moreover, treatment with MOG and IFA did not induce EAE symptoms (15,18). These data suggest that IL-6 induced by CFA plays important roles in the pathogenesis of autoimmune diseases. However, the relative contributions of the SSc-specific antigen, topo I, and IL-6 induced by CFA to the development of SSc remain unknown.

In this study, we investigated the associations of topo I immunization and of IL-6 induced by CFA with the development of SSc, using wild-type (WT) and IL-6–deficient (IL-$6^{-/-}$) mice. According to our results, treatment with both topo I and CFA increased IL-6 and IL-17 production and Th17 cell frequencies compared to treatment with both topo I and IFA. In contrast, IL-10 production and Treg cell frequencies were greater in WT mice treated with topo I and IFA than in WT mice treated with topo I and CFA. Furthermore, treatment with topo I and CFA induced dermal sclerosis, pulmonary fibrosis, and anti–topo I antibody production, although treatment with topo I and IFA induced only anti–topo I antibody production. In addition, IL-6 deficiency reduced dermal sclerosis, pulmonary fibrosis, and IL-17 and anti–topo I antibody production as well as the increased Th17 cell frequencies induced by treatment with topo I and CFA, while increasing IL-10 production and Treg cell frequencies. These results suggest that subcutaneous treatment with topo I and CFA induces dermal sclerosis, pulmonary fibrosis, and autoimmune abnormalities, which are mainly regulated by IL-6.

MATERIALS AND METHODS

Mice. WT C57BL/6 mice and IL-$6^{-/-}$ mice with a C57BL/6 background were purchased from The Jackson Laboratory. All mice were housed in a specific pathogen–free barrier facility and screened regularly for pathogens. The mice used in these experiments were age 6 weeks. All studies and procedures were approved by the Committee on Animal Experimentation of Nagasaki University Graduate School of Biomedical Sciences.

Topo I and/or adjuvant treatment. Recombinant human topo I (TopoGEN) was dissolved in saline (500 units/ml). The topo I solution was mixed 1:1 (volume/volume) with CFA H37Ra (Sigma-Aldrich) or IFA (Sigma-Aldrich). These solutions (300 μl) were injected 4 times subcutaneously into a single location on the shaved back of the mice with a 26-gauge needle at an interval of 2 weeks. Human serum albumin (Protea Biosciences) was used as an irrelevant control human protein, as previously described (19–21). Treatment with human serum albumin with or without adjuvant did not affect skin and lung fibrosis, cytokine production, autoantibody production, or Th cell frequencies in bronchoalveolar lavage (BAL) fluid.

Histopathologic assessment of dermal fibrosis. Morphologic characteristics of skin sections were assessed under a light microscope. All skin sections were obtained from the paramidline, lower back region (the same anatomic site, to minimize regional variations in thickness). Sections were stained with hematoxylin and eosin (H&E). Dermal thickness, defined as the thickness of skin from the top of the granular layer to the junction between the dermis and subcutaneous fat, was examined. Ten random measurements per section were obtained. All of the sections were examined independently by 2 investigators (AY and SS) in a blinded manner.

Histopathologic assessment of lung fibrosis. Lungs were excised after 4 weeks of treatment and processed as previously described (12,13). Sections were stained with H&E and with Azan-Mallory stain to identify collagen deposition. The severity of fibrosis was semiquantitatively assessed according to the method described by Ashcroft et al (22). Briefly, lung fibrosis was graded on a scale of 0 to 8 by examining randomly chosen fields of the left middle lobe. The grading criteria were as follows: grade 0 = normal lung; grade 1 = minimal fibrous thickening of alveolar walls; grade 3 = moderate thickening of walls without obvious damage; grade 5 = increased fibrosis with definite damage and formation of fibrous bands; grade 7 = severe distortion of structure and large fibrous areas; and grade 8 = total fibrous obliteration. Grades 2, 4, and 6 were used as intermediate stages between these criteria. In addition, apoptotic cells were examined using

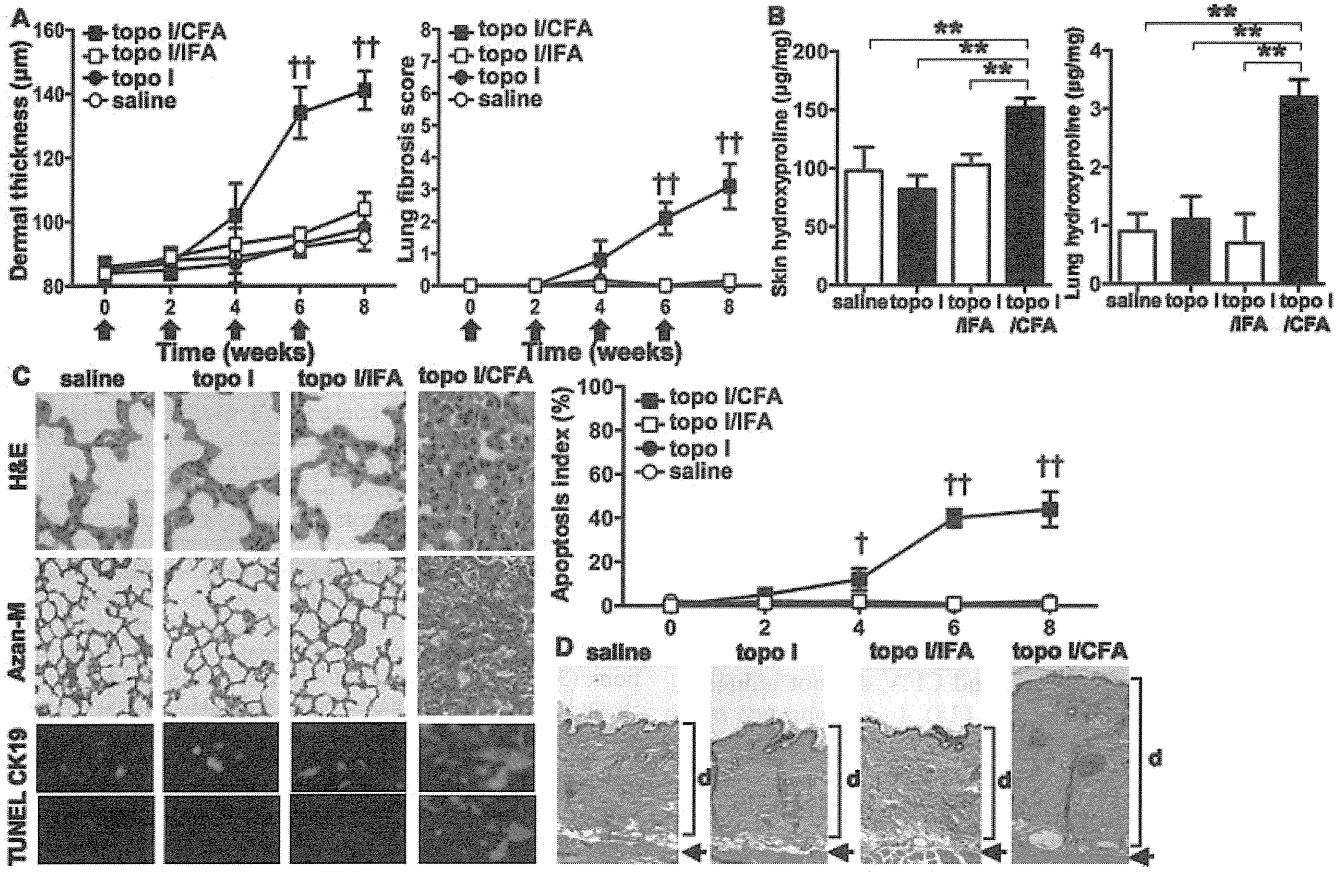

Figure 1. Skin and lung fibrosis in wild-type (WT) mice treated with saline, DNA topoisomerase I (topo I) alone, topo I and Freund's incomplete adjuvant (IFA), or topo I and Freund's complete adjuvant (CFA). **A** and **B,** Skin and lung fibrosis was assessed by quantitatively measuring dermal thickness and the lung fibrosis score 0, 2, 4, 6, and 8 weeks after treatment (**A**) and skin and lung hydroxyproline content 8 weeks after treatment (**B**). Each **arrow** in **A** indicates a single treatment. **C,** Shown are representative lung histologic sections obtained after 8 weeks of treatment, stained with hematoxylin and eosin (H&E) (original magnification × 200), Azan-Mallory stain (Azan-M) (original magnification × 40), and TUNEL (red fluorescence) (original magnification × 400). Cytokeratin 19 (CK19; green fluorescence) (original magnification × 400) was used to determine the presence of alveolar epithelial cells. Also shown is the apoptosis index. **D,** Shown are representative skin histologic sections obtained after 8 weeks of treatment, stained with H&E (original magnification × 40). **d** indicates dermis; **arrow** indicates hypodermis beneath the panniculus carnosus. The hypodermal thickness was measured under a light microscope. Each histogram shows the mean ± SD results obtained for 10 mice of each group. † = $P < 0.05$; †† = $P < 0.01$ versus WT mice treated with saline or topo I alone. ** = $P < 0.01$.

the TUNEL assay (Oncor) according to the manufacturer's instructions. Fluorescein isothiocyanate (FITC; green fluorescence)–labeled antidigoxigenin conjugate was applied to detect apoptotic cells. Phycoerythrin (PE; red fluorescence)–conjugated anti–cytokeratin 19 monoclonal antibody (mAb) was used to detect alveolar epithelial cells. These slides were visualized with a fluorescence microscope (Olympus). The percentage of apoptotic epithelial cells was referred to as the apoptosis index, as described previously (23).

Determination of hydroxyproline content in skin and lung tissue. Hydroxyproline is a modified amino acid uniquely found at a high percentage in collagen. Therefore, the skin and lung tissue hydroxyproline content was determined as a quantitative measure of collagen deposition (24). Punch biopsy samples (6 mm) obtained from the shaved dorsal skin and the harvested right lung of each mouse were analyzed. A hydroxyproline standard solution of 0–6 mg/ml was used to generate a standard curve.

Enzyme-linked immunosorbent assay (ELISA) for serum cytokines, immunoglobulins, and autoantibodies. Serum levels of IL-4, IL-6, IL-10, IL-17, interferon-γ (IFNγ), TGFβ1, and tumor necrosis factor α (TNFα) were assessed using specific ELISA kits (R&D Systems). Serum Ig concentrations were assessed as described (13), using affinity-purified mouse IgM, IgG1, IgG2a, IgG2b, IgG3, and IgA (SouthernBiotech) to generate standard curves. ANAs were assessed by indirect immunofluorescence staining using HEp-2 substrate cells (Medical & Biological Laboratories) as described (13). The specific ELISA kits were used to measure anti–topo I (Medical & Biological Laboratories), anti–CENP B (Funakoshi), and

anti–U1 RNP antibody (Medical & Biological Laboratories). Relative levels of these antibodies were determined for each group of mice, using pooled serum samples. Sera were diluted at log intervals (1:10–1:10^5) and assessed for relative autoantibody levels as above, except that the results were plotted as optical density (OD) versus dilution (log scale). The dilutions of sera giving half-maximal OD values were determined by linear regression analysis, thus generating arbitrary units per milliliter values for comparison between sets of sera.

RNA isolation and real-time polymerase chain reaction (PCR). Total RNA was isolated from lower back skin and lung with RNeasy spin columns (Qiagen). Expression of IL-4, IL-6, IL-10, IL-17, IFNγ, TGFβ1, and TNFα was analyzed by TaqMan Assay (Applied Biosystems). GAPDH was used to normalize messenger RNA (mRNA). Relative expression of real-time PCR products was determined using the $\Delta\Delta C_t$ method (13).

Preparation of BAL fluid. BAL fluid cells were prepared as described elsewhere (25). Briefly, both lungs were excised from mice and BAL fluid was collected. T cells were enriched with a mouse CD4+ T cell kit using an AutoMacs isolator (Miltenyi Biotec). More than 99% of these cells were CD4+ when tested with anti-CD4 mAb (Serotec) (data not shown).

Flow cytometry. Antibodies used in this study included FITC-conjugated anti-mouse mAb to IL-4 (Imgenex), IFNγ (Genetex), IL-17 (Novus Biologicals), and FoxP3 (Lifespan Biosciences) as well as PE-conjugated anti-mouse mAb to CD4 (Serotec). IFNγ, IL-4, IL-17, and FoxP3 production by BAL fluid CD4+ T cells was determined by flow cytometric intracellular cytokine analysis, as previously described (26,27). All intracellular staining samples were stimulated with phorbol myristate acetate (50 ng/ml; Sigma-Aldrich) and ionomycin (500 ng/ml; Sigma-Aldrich) for 5 hours before analysis.

Statistical analysis. All data are expressed as the mean ± SD. The Mann-Whitney U test was used to determine the level of significance of differences between sample means, and analysis of variance followed by Bonferroni adjustment was used for multiple comparisons.

RESULTS

Subcutaneous injection of topo I and CFA induces dermal sclerosis and pulmonary fibrosis. Skin and lung fibrosis was histopathologically assessed 2, 4, 6, and 8 weeks after the initiation of topo I treatment. The dermal thickness and lung fibrosis score increased in a time-dependent manner in mice treated with topo I and CFA (Figure 1). Skin fibrosis, lung fibrosis, alveolar epithelial apoptosis, and inflammatory cell infiltration developed during the first 8 weeks of treatment with

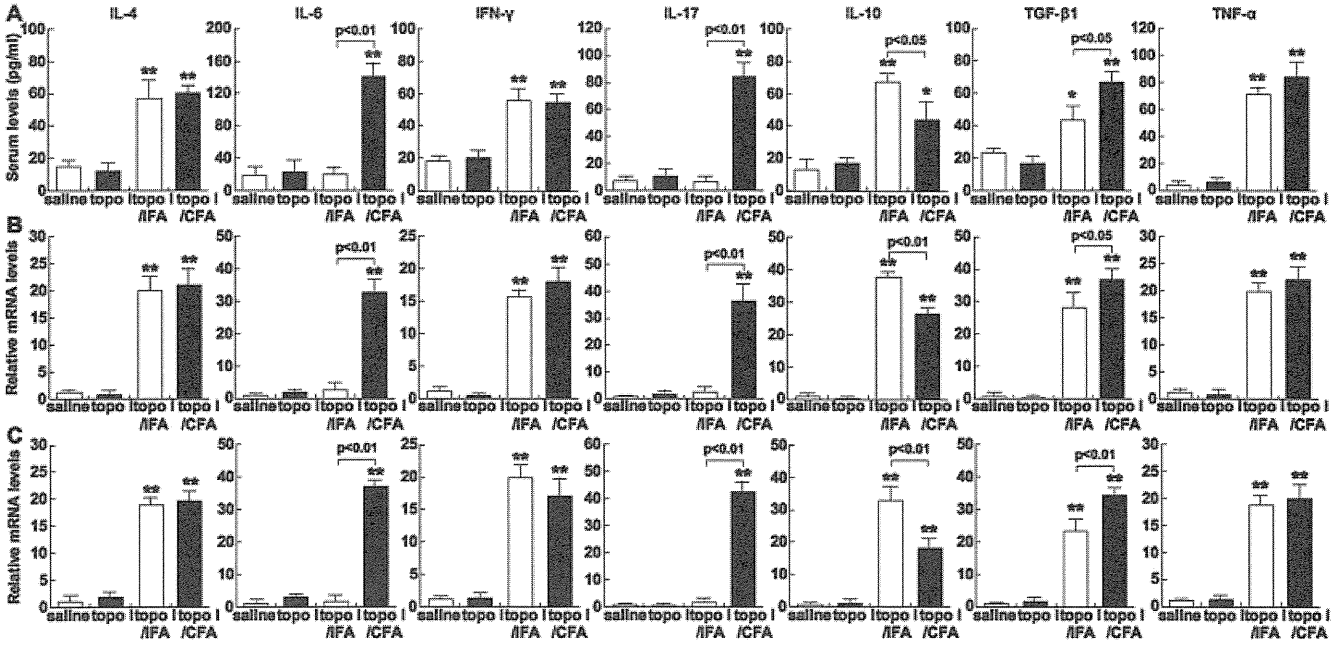

Figure 2. Levels of interleukin-4 (IL-4), IL-6, interferon-γ (IFNγ), IL-17, IL-10, transforming growth factor β1 (TGFβ1), and tumor necrosis factor α (TNFα) in serum samples (**A**) and their mRNA expression in the skin (**B**) and lung (**C**) from WT mice treated with saline, topo I alone, topo I and IFA, or topo I and CFA. Serum samples were obtained by cardiac puncture 8 weeks after treatment. Serum cytokine levels were assessed using specific enzyme-linked immunosorbent assays. Total RNA from lower back skin and lung was extracted and reverse transcribed to cDNA, and mRNA expression was analyzed using real-time polymerase chain reaction and normalized to the internal control GAPDH. Each histogram shows the mean ± SD results obtained for 10 mice of each group. * = $P < 0.05$; ** = $P < 0.01$ versus WT mice treated with saline or topo I alone. See Figure 1 for other definitions.

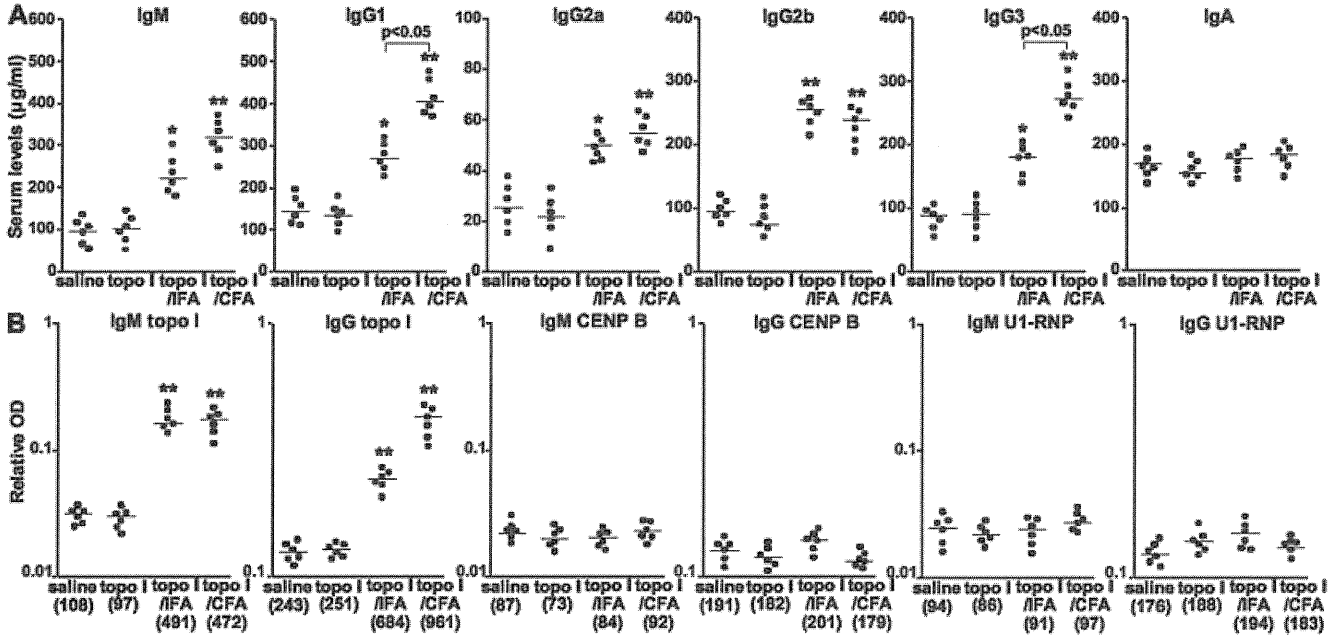

Figure 3. Serum levels of immunoglobulins (**A**) and autoantibodies (**B**) in WT mice treated with saline, topo I alone, topo I and IFA, or topo I and CFA. Serum samples were obtained by cardiac puncture 8 weeks after treatment. Serum levels of immunoglobulins and autoantibodies were determined by specific enzyme-linked immunosorbent assays (ELISAs). Horizontal bars represent the mean. Values in parentheses represent the dilutions of pooled sera giving half-maximal optical density (OD) values in anti–topo I, anti–CENP B, and anti–U1 RNP antibody ELISAs, which were determined by linear regression analysis to generate arbitrary units per ml that could be directly compared between each group of mice (n = 6 for each). $* = P < 0.05$; $** = P < 0.01$ versus WT mice treated with saline or topo I alone. See Figure 1 for other definitions.

topo I and CFA, peaked in the eighth week (Figure 1A), and began to resolve 6 weeks after the cessation of treatment (data not shown). After 6 weeks, treatment with topo I and CFA induced significantly greater dermal thickness relative to saline treatment in WT mice ($P < 0.01$), although there was no significant difference in dermal thickness among mice treated with saline, topo I, and topo I with IFA (Figures 1A and D). In addition, the dermal thickness was similar among untreated mice, saline-treated mice, IFA-treated mice, and CFA-treated mice. Furthermore, there was no significant difference in dermal thickness and inflammatory cell infiltration between the injected site and the other site.

Similar results were obtained for the lung fibrosis score and apoptosis index (Figures 1A and C). After 8 weeks of topo I administration, WT mice treated with topo I and CFA exhibited extensive inflammatory infiltration, diffuse fibrosis, and alveolar epithelial apoptosis. Topo I treatment with or without IFA did not affect the development of lung fibrosis and epithelial apoptosis. Cutaneous and lung fibrosis was also assessed by quantifying the hydroxyproline content. In mice treated with topo I and CFA, the skin and lung hydroxyproline content was significantly increased compared with that in mice treated with saline, topo I, or topo I with IFA ($P < 0.01$ for all) (Figure 1B).

Topo I and adjuvant treatment together induce overproduction of cytokines in the serum, skin, and lung. In the serum (Figure 2A), skin (Figure 2B), and lung (Figure 2C), mice treated with topo I and CFA or topo I and IFA had elevated levels of IL-4, IFNγ, IL-10, TGFβ1, and TNFα compared with mice treated with saline or topo I alone ($P < 0.05$ for all). Serum, skin, and lung levels of TGFβ1 were higher in mice treated with topo I and CFA than in mice treated with topo I and IFA ($P < 0.05$ for all), while mice treated with topo I and IFA showed increased levels of IL-10 relative to mice treated with topo I and CFA ($P < 0.05$ for all). Mice treated with topo I and CFA exhibited elevated levels of IL-6 and IL-17 compared with mice treated with saline, topo I, or topo I with IFA ($P < 0.01$ for all).

Elevated serum Ig and anti–topo I antibody levels in mice treated with both topo I and adjuvant. WT mice treated with topo I alone had Ig levels similar to those in saline-treated WT mice. Treatment with both topo I and adjuvant increased serum IgM, IgG1, IgG2a,

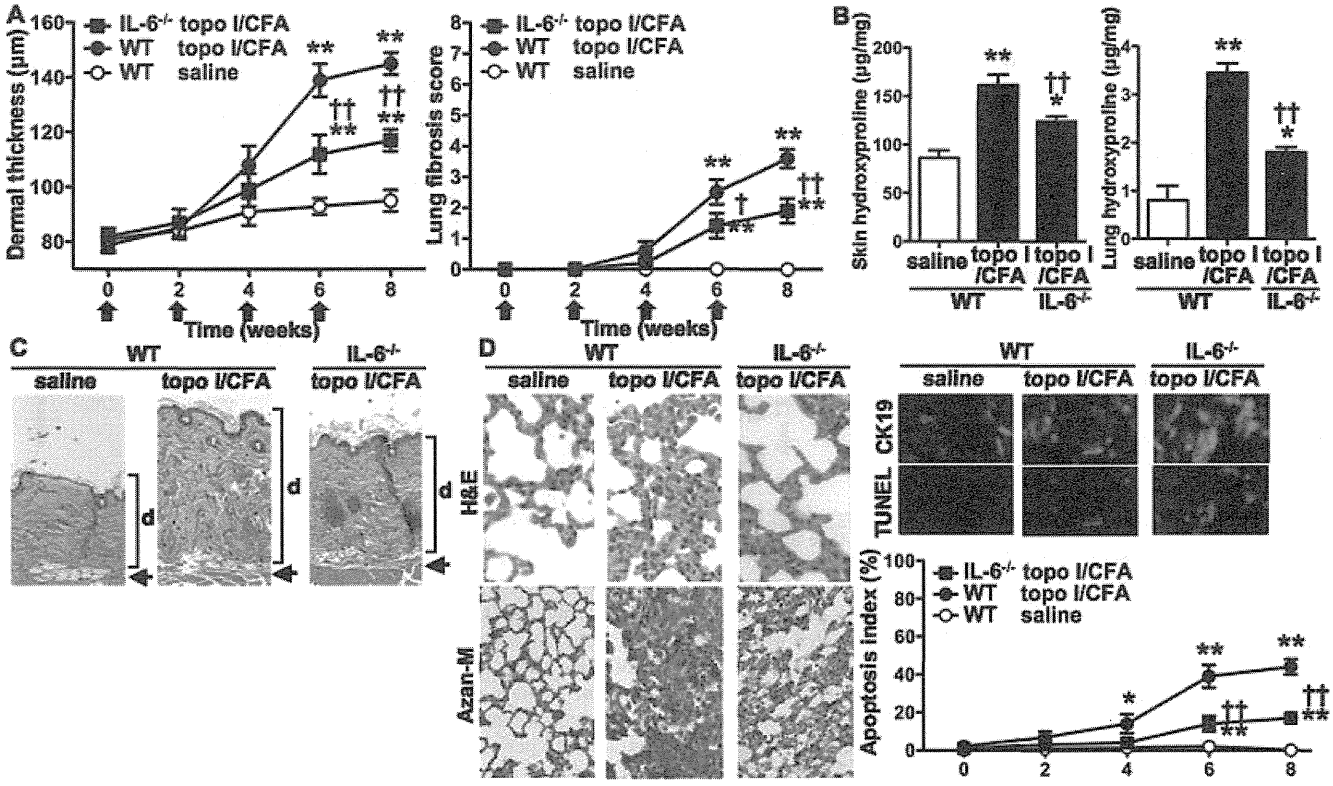

Figure 4. Skin and lung fibrosis in WT mice treated with saline or with topo I and CFA, and in interleukin-6–deficient (IL-$6^{-/-}$) mice treated with topo I and CFA. **A** and **B,** Skin and lung fibrosis was assessed by quantitatively measuring dermal thickness and the lung fibrosis score 0, 2, 4, 6, and 8 weeks after treatment (**A**) and skin and lung hydroxyproline content 8 weeks after treatment (**B**). Each **arrow** in **A** indicates a single treatment. **C,** Shown are representative skin histologic sections obtained after 8 weeks of treatment, stained with H&E (original magnification × 40). **d** indicates dermis; **arrow** indicates hypodermis beneath the panniculus carnosus. **D,** Shown are representative lung histologic sections obtained after 8 weeks of treatment, stained with H&E (original magnification × 200), Azan-Mallory stain (original magnification × 40), and TUNEL (red fluorescence) (original magnification × 400). Cytokeratin 19 (green fluorescence) (original magnification × 400) was used to determine the presence of alveolar epithelial cells. Also shown is the apoptosis index. Each histogram shows the mean ± SD results obtained for 10 mice of each group. † = $P < 0.05$; †† = $P < 0.01$ versus WT mice treated with topo I and CFA. * = $P < 0.05$; ** = $P < 0.01$ versus saline-treated WT mice. See Figure 1 for other definitions.

IgG2b, and IgG3 levels compared with saline treatment ($P < 0.05$ for all) (Figure 3A), while the levels of IgA were similar between mice treated with both topo I and adjuvant and saline-treated mice. Mice treated with topo I and CFA had increased IgG1 and IgG3 levels compared with mice treated with topo I and IFA ($P < 0.05$ for both), while there were no significant differences in the levels of other isotypes between mice treated with topo I and IFA and mice treated with topo I and CFA. ANAs were rarely detectable in saline-treated mice and mice treated with topo I alone (5% of mice, or 1 in 20). ANAs with a homogeneous chromosomal staining pattern were detected in 84% of mice (27/32) treated with topo I and CFA, which was similar to the percentage in mice treated with topo I and IFA (78% [25/32]).

Autoantibody specificities were further assessed by ELISA (Figure 3B). Mice treated with both topo I and adjuvant had increased levels of IgM and IgG autoantibodies to topo I relative to saline-treated mice and mice treated with topo I alone ($P < 0.01$ for both). Furthermore, IgG anti–topo I antibody production in mice treated with topo I and CFA was greater than that in mice treated with topo I and IFA ($P < 0.05$). In addition, the levels of anti–topo I antibody increased during the first 8 weeks of treatment with topo I and CFA, peaked in the eighth week, and began to resolve 6 weeks after the cessation of treatment. Treatment with saline, topo I alone, topo I with CFA, or topo I with IFA did not affect levels of autoantibodies to CENP B and U1 RNP.

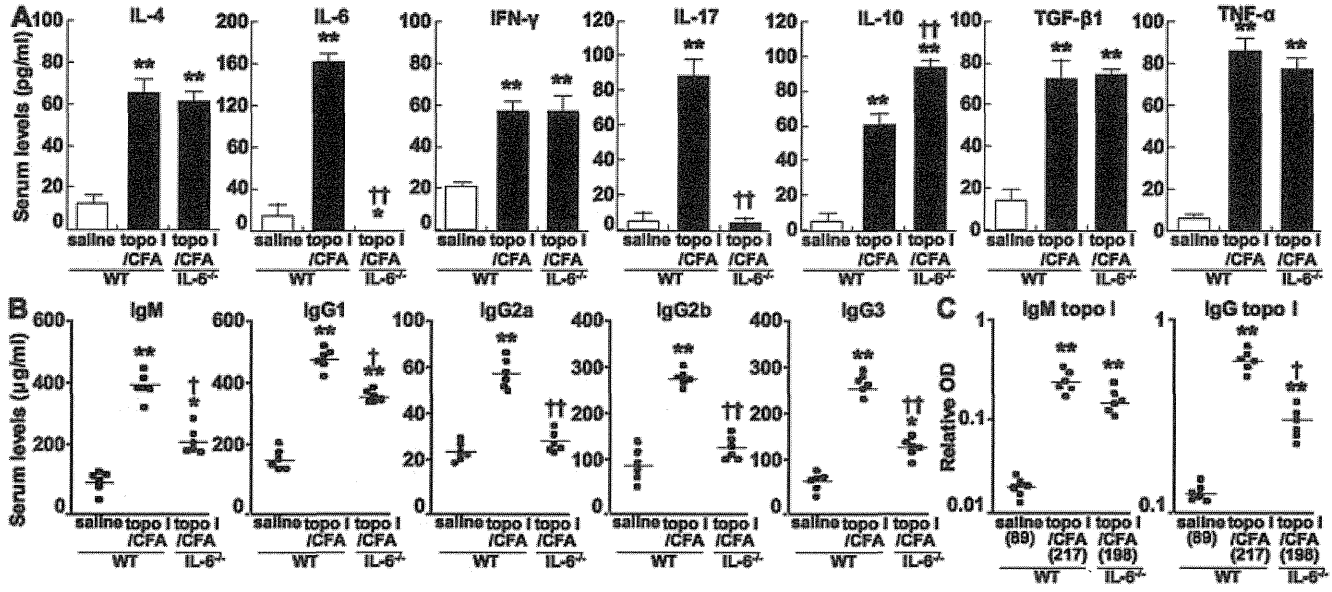

Figure 5. Serum levels of cytokines (**A**), immunoglobulins (**B**), and anti–topo I antibodies (**C**) in WT mice treated with saline or with topo I and CFA, and in interleukin-6–deficient (IL-$6^{-/-}$) mice treated with topo I and CFA. Serum samples were obtained by cardiac puncture 8 weeks after treatment. Serum levels of cytokines, immunoglobulins, and anti–topo I antibodies were determined by specific enzyme-linked immunosorbent assays (ELISAs). In **A,** each histogram shows the mean ± SD results obtained for 10 mice of each group. In **B** and **C,** horizontal bars represent the mean. In **C,** values in parentheses represent the dilutions of pooled sera giving half-maximal optical density (OD) values in anti–topo I antibody ELISAs, which were determined by linear regression analysis to generate arbitrary units per ml that could be directly compared between each group of mice (n = 6 for each). † = $P < 0.05$; †† = $P < 0.01$ versus WT mice treated with topo I and CFA. * = $P < 0.05$; ** = $P < 0.01$ versus saline-treated WT mice. IFNγ = interferon-γ; TGFβ1 = transforming growth factor β1; TNFα = tumor necrosis factor α (see Figure 1 for other definitions).

IL-6 loss attenuates the development of skin and lung fibrosis induced by treatment with topo I and CFA. In IL-$6^{-/-}$ mice treated with topo I and CFA, skin fibrosis, lung fibrosis, and epithelial apoptosis similar to that in WT mice treated with topo I and CFA developed during the first 8 weeks of treatment with topo I and CFA and peaked in the eighth week (Figure 4). However, after 6 and 8 weeks, IL-$6^{-/-}$ mice treated with topo I and CFA showed moderate thickening of dermal tissue that was significantly less (31% and 32%, respectively) than that found in WT mice treated with topo I and CFA ($P < 0.01$), but still greater than that in saline-treated WT mice ($P < 0.01$) (Figures 4A and C). Saline-treated WT and IL-$6^{-/-}$ mice showed similar dermal thickness (data not shown). Similar results were obtained for the lung fibrosis score and apoptosis index (Figures 4A and D). After 8 weeks, WT mice treated with topo I and CFA exhibited extensive inflammatory cell infiltration, fibrosis, and alveolar epithelial apoptosis. IL-6 deficiency reduced such histologic changes. Skin and lung fibrosis was also assessed by quantifying hydroxyproline content. The skin and lung hydroxyproline content in IL-$6^{-/-}$ mice treated with topo I and CFA was significantly lower than that in WT mice treated with topo I and CFA ($P < 0.01$), but the content remained higher than that in saline-treated WT mice ($P < 0.05$) (Figure 4B).

IL-6 deficiency suppresses overproduction of cytokines, Ig, and autoantibodies induced by treatment with topo I and CFA. Serum levels of IL-6 were not detected in IL-$6^{-/-}$ mice (Figure 5A). Furthermore, there was no difference in serum levels of IL-4, IFNγ, IL-17, IL-10, TGFβ1, and TNFα between saline-treated IL-$6^{-/-}$ mice and saline-treated WT mice. In contrast, 8 weeks after treatment with topo I and CFA, serum levels of all cytokines examined were increased in WT mice ($P < 0.01$). However, IL-$6^{-/-}$ mice showed a significant decrease in serum IL-17 levels relative to WT mice ($P < 0.01$). In contrast, IL-$6^{-/-}$ mice showed significantly increased production of IL-10 relative to WT littermates ($P < 0.01$). Similar results were obtained for skin and lung mRNA expression (data not shown). Furthermore, IL-$6^{-/-}$ mice treated with topo I and CFA showed significantly lower levels of IgM, IgG1, IgG2a, IgG2b,

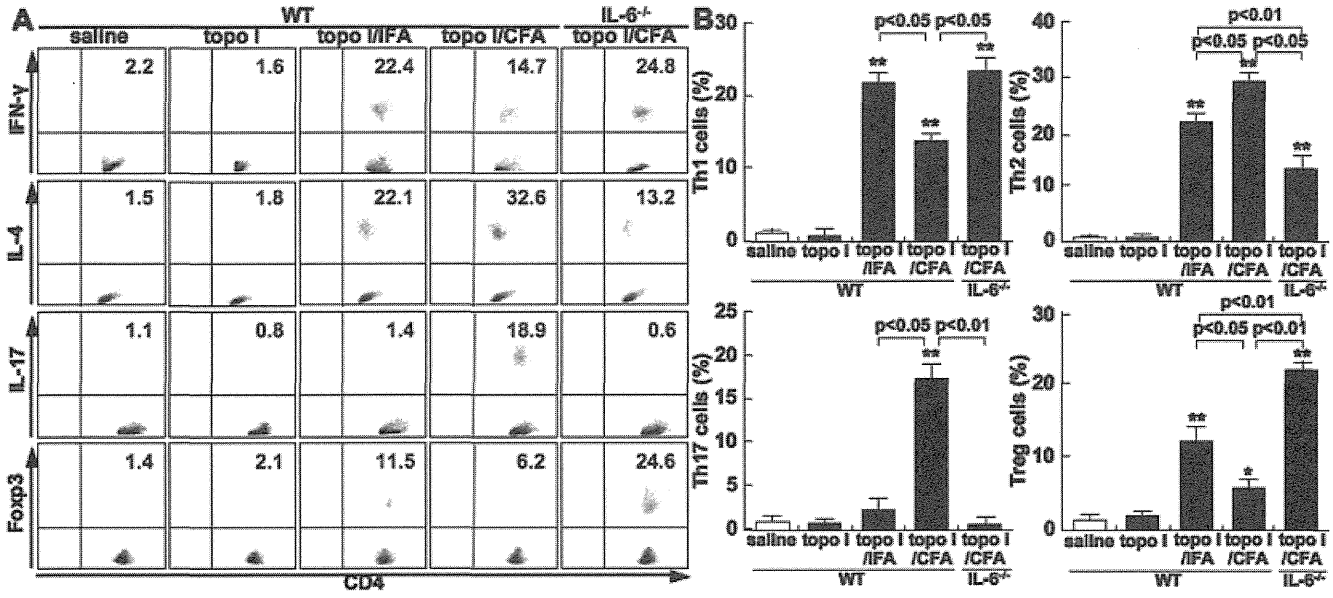

Figure 6. Th1, Th2, Th17, and Treg cell frequencies in bronchoalveolar lavage (BAL) fluid from WT mice treated with saline, topo I alone, topo I and IFA, or topo I and CFA, and from interleukin-6–deficient (IL-$6^{-/-}$) mice treated with topo I and CFA. **A,** Th1, Th2, Th17, and Treg cell frequencies were determined by surface CD4 expression and intracellular expression of interferon-γ (IFNγ), IL-4, IL-17, and FoxP3, respectively, as previously described (26). BAL fluid was analyzed by flow cytometry after 8 weeks of topo I or saline treatment. Data are representative of 3 independent experiments. Percentages of Th1, Th2, Th17, and Treg cells are shown in each upper right quadrant. **B,** Shown are summaries of Th1, Th2, Th17, and Treg cell frequencies in each group. Each histogram shows the mean ± SD results obtained for 10 mice of each group. * = $P < 0.05$; ** = $P < 0.01$ versus WT mice treated with saline or topo I alone. See Figure 1 for other definitions.

and IgG3 compared with WT mice treated with topo I and CFA ($P < 0.05$), but these levels remained higher than those in saline-treated WT mice (Figure 5B). Serum levels of autoantibodies were also examined (Figure 5C). IL-$6^{-/-}$ mice treated with topo I and CFA had decreased levels of IgG autoantibodies to topo I compared with WT mice treated with topo I and CFA ($P < 0.05$).

Th cell balance in BAL fluid from mice treated with saline, topo I alone, or both topo I and adjuvant. We investigated Th1, Th2, Th17, and Treg cell frequencies in BAL fluid from WT mice treated with saline, topo I alone, topo I and IFA, or topo I and CFA, and from IL-$6^{-/-}$ mice treated with topo I and CFA (Figure 6). The percentages of CD4+ BAL fluid cells were 15.2%, 14.9%, 16.7%, 15.8%, and 15.4% in saline-treated WT mice, WT mice treated with topo I alone, WT mice treated with topo I and IFA, WT mice treated with topo I and CFA, and IL-$6^{-/-}$ mice treated with topo I and CFA, respectively. The populations expressing IFNγ, IL-4, IL-17, or FoxP3 did not overlap (data not shown), which is consistent with previous studies (26).

There were no significant differences in Th1, Th2, Th17, and Treg cell frequencies between saline-treated WT mice and WT mice treated with topo I alone. WT mice treated with topo I and IFA exhibited significantly increased Th1, Th2, and Treg cell frequencies compared with saline-treated WT mice ($P < 0.01$ for all). Similarly, WT mice treated with topo I and CFA exhibited significantly increased frequencies of Th1 cells ($P < 0.01$), Th2 cells ($P < 0.01$), Th17 cells ($P < 0.01$), and Treg cells ($P < 0.05$) relative to saline-treated WT mice. In addition, Th1 and Treg cell frequencies were significantly lower in WT mice treated with topo I and CFA than in WT mice treated with topo I and IFA ($P < 0.05$ for both). Moreover, WT mice treated with topo I and CFA displayed higher frequencies of Th2 and Th17 cells compared with WT mice treated with topo I and IFA ($P < 0.05$ for both). IL-$6^{-/-}$ mice treated with topo I and CFA exhibited significantly increased frequencies of Th1, Th2, and Treg cells compared with saline-treated WT mice. Furthermore, Th1 and Treg cell frequencies were significantly increased in IL-$6^{-/-}$ mice treated with topo I and CFA compared with WT mice treated with topo I and CFA ($P < 0.05$ and $P < 0.01$, respectively). In contrast, IL-$6^{-/-}$ mice treated with topo I and CFA exhibited significantly reduced Th2 and Th17 cell frequencies compared with WT mice treated with topo I and CFA ($P < 0.05$ and $P < 0.01$, respectively).

DISCUSSION

The precise mechanisms involved in the pathogenesis of SSc remain unknown, although autoimmunity is considered to be involved (3). The presence of anti–topo I antibody has been clinically associated with a more severe form of SSc that exhibits diffuse cutaneous and lung involvement (3,9,10,28). In addition, a recent study showed that 20% of anti–topo I antibody–positive patients lost anti–topo I antibodies during the disease course and had a favorable outcome, suggesting the clinical importance of anti–topo I antibody levels in patients with SSc (29). The topo I protein is a ubiquitous and indispensable enzyme involved in DNA replication and protein transcription (30). Human topo I has >93% sequence identity to the 766 amino acid residues of mouse topo I (GenBank accession no. L20632). It has been demonstrated that immunization using a mutated self antigen is capable of inducing an autoreactive response that is more potent than that using the bona fide autoantigen in mice (31). Therefore, we immunized mice with recombinant human topo I as described previously (14,32). The present study is the first to demonstrate that subcutaneous injection of topo I with CFA induces skin and lung fibrosis, hypergammaglobulinemia, and anti–topo I antibody production in WT mice (Figures 1 and 3), generating many characteristics of human SSc. Furthermore, treatment with topo I and CFA increased the production of various fibrogenic cytokines (Figure 2). Collectively, these results indicate that mice treated with topo I and CFA show SSc-like fibrosis and might be a novel animal model of human SSc.

In this study, treatment with topo I and IFA, in contrast to treatment with topo I and CFA, did not induce skin and lung fibrosis (Figure 1). Previous studies have demonstrated that CFA is essential for development of autoimmune responses, such as autoimmune encephalomyelitis, in each of the induction protocols (18). In contrast, IFA injection can prevent induction by CFA (33). This may be explained by the fact that CFA treatment induces IL-6 production, whereas IFA injection cannot affect IL-6 production (15,34,35). Indeed, in our present study, WT mice treated with topo I and CFA exhibited significantly higher levels of IL-6 relative to mice treated with topo I and IFA (Figure 2). Moreover, a recent study has shown that both IL-6 induced by CFA and exogenous IL-6 injection augment autoantibody production in immunized mice (36). In the present study, the levels of IgG anti–topo I antibody, IgG1, and IgG3 in WT mice treated with topo I and CFA were greater than those in WT mice treated with topo I and IFA (Figure 3). These results suggest that IL-6 induced by CFA contributes to development of fibrosis and augments autoantibody production. Furthermore, a recent case report has shown that the anti–IL-6 receptor antibody tocilizumab decreased skin sclerosis in SSc patients (37). In fact, IL-6 deficiency inhibited the development of fibrosis with decreased autoantibody production in mice treated with topo I and CFA (Figures 4 and 5). Thus, immunization with topo I can induce dermal and pulmonary fibrosis and hypergammaglobulinemia, which requires IL-6 induced by CFA.

Previous studies have demonstrated a fibrogenic effect of Th2 cytokines, such as IL-4 and IL-6 (13,24,38). Th17 cytokines, such as IL-17, also have a fibrogenic effect on dermal, pulmonary, and cardiac fibroblasts (39,40). Indeed, SSc patients exhibit elevated serum levels of these cytokines, which promote collagen synthesis (5,6,27,39,41,42). Some studies have also shown that IFNγ, a Th1 cytokine, has an antifibrotic effect (26,27,43,44). In addition, IL-10 produced by Treg cells has antifibrotic and antiinflammatory effects on fibrotic diseases (45). Previously, we and others confirmed that IL-4 and/or IL-17 stimulation increased proliferation and collagen production of dermal fibroblasts, while these processes were inhibited by IFNγ and IL-10 (27,45). The results of the present study indicate differential expression levels of these cytokines in mice treated with both topo I and adjuvant (Figure 2). Treatment with topo I and CFA induced significantly higher production of IL-6, IL-17, and TGFβ1 in parallel with increased dermal and pulmonary fibrosis. Treatment with topo I and IFA enhanced IL-10 production, which was accompanied by inhibited fibrosis. Thus, the differential expression levels of these cytokines that were induced by topo I and adjuvant treatment might contribute to the development of skin and lung fibrosis.

It is possible that treatment with topo I and adjuvant alters the frequencies of fibrogenic Th2 and Th17 cells and antifibrogenic Th1 and Treg cells. This may result in differential production of cytokines, which may then directly or indirectly influence the development of dermal sclerosis, pulmonary fibrosis, and autoimmune abnormalities. A recent study indicated that CD4+ cells play an important role in fibrosis, although these cells are a minority population (27). Moreover, previous studies have demonstrated that IL-6 together with TGFβ1 is capable of inducing Th17 cells (15). Furthermore, in the absence of IL-6, Th17 cell responses are impaired, whereas Treg cell responses are dominant, suggesting that IL-6 is a critical factor that shifts the